Spring 5-2020

Applications of Digital Remote Sensing to Quantify Glacier Change in Glacier and Mount Rainier National Parks

Brianna Clark
clarkbm@jacks.sfasu.edu

Applications of Digital Remote Sensing to Quantify Glacier Change

in Glacier and Mount Rainier National Parks

By

BRIANNA MARIE CLARK, Bachelor of Arts

Presented to the Faculty of the Graduate School of

Stephen F. Austin State University

In Partial Fulfillment

of the Requirements

For the Degree of

Master of Science

STEPHEN F. AUSTIN STATE UNIVERSITY

May, 2020

ABSTRACT

Digital remote sensing and geographic information systems were employed in performing area and volume calculations on glacial landscapes. Characteristics of glaciers from two geographic regions, the Intermountain Region (between the Rocky Mountain and Cascade Ranges) and the Pacific Northwest, were estimated for the years 1985, 2000, and 2015. Glacier National Park was studied for the Intermountain Region whereas Mount Rainier National Park was representative of the glaciers in the Pacific Northwest. Within the thirty year period of the study, the glaciers in Glacier National Park decreased in area by 27.5 percent while those on Mount Rainier only decreased by 5.7 percent. The differences in these percentages can be attributed to the warmer temperatures of the Intermountain Region coupled with lower amounts of snowfall when compared to the Pacific Northwest. Volume loss calculations were also performed, but digital remote sensing and GIS were less successful at estimating this glacial parameter.

TABLE OF CONTENTS

LIST OF FIGURES

LIST OF TABLES

INTRODUCTION

Glaciers, a significant aspect of the cryosphere, are highly interwoven into the Earth's processes. Both anthropological and natural factors contribute to the extent of the cryosphere. Eleven percent of Earth's land area is covered by glaciers or ice sheets, and store approximately 75 percent of the world's fresh water (Pellikka and Rees, 2010; NSIDC, 2019). In 1998, it was predicted that a third to a half of the existing glacier mass would disappear by 2100 and that the global temperature would increase by 4° Celsius; temperate glaciers were believed to be decreasing in depth by one to two meters a year (Haeberli and Beniston, 1998). The Randolph Glacier Inventory lists 198,000 glaciers worldwide (excluding ice sheets), however it is recognized that this quantity is arbitrary (Davies, 2017). A recent study estimated there to be closer to 215,000 glaciers, excluding ice sheets (Farinotti et al., 2019). The lack of a precise number of glaciers highlights the difficulty of performing glacier calculations.

A field that was once limited by available transportation and finances, glaciology has radically expanded due to the development of satellites dedicated to surveying the Earth. Once unobtainable for study, remote glaciers are available for analyses through both current and historic satellite imagery. Non-geodetic forms of glacier monitoring involved scientific excursions to glaciers and the placement of stakes. Return trips in following seasons and years allowed for calculations in glacier position and size relative to the locations of the monitoring stakes. Due to the remote locations of glaciers, expeditions are not always cost efficient or possible. In addition to being potentially cheaper, satellite remote sensing allows glaciologists to go back in time and access imagery from years previous. Parameters that can be measured using satellite remote sensing include equilibrium line altitudes, volumes, mass balances, and glacier area calculations, which previously were not accurately able to be performed. Using these calculations, the ablation rate can be estimated and models of future glacier extents developed. The data derived from satellite remote sensing is being compiled into databases such as those provided by the World Glacier Monitoring Service (WGMS), Global Land Ice Measurements from Space (GLIMS), and as part of the OMEGA project which is intended to serve as a monitoring system (Pellikka and Rees, 2010).

Interest in glaciers goes beyond academia, as it is a topic for policymakers and political leaders. Glaciers serve as important indicators of climate change. They fluctuate in size as a response to global temperature and precipitation trends. Glaciers are valuable, in part, due to their widespread distribution. Developing good methods for glacial calculations is crucial to the early detection of climate change. In addition to serving as a warning system for changes in the Earth's conditions, glaciers demand attention for their meltwater. Economies are fueled by hydraulic power produced by melting glaciers. Communities use glacial melt as one of their main sources of drinking water. Glaciers are linked to the hydrosphere with many rivers having their origins from glaciers and the meltwater feeding into coastal ecosystems. If a glacier is completely lost from an environment, then all of its contributions to the hydrologic cycle are likewise lost. The melting of glaciers also poses risks of avalanches, floods, and upsets to the sequestration of gases in permafrost. In 2002, an ice rock avalanche in the Caucasus killed approximately 140 people; disasters such as this are a grim reminder as to why there is a need to continuously monitor and study glaciers (WGMS, 2008).

In recent years, there have been numerous articles and books published discussing the use of remote sensing in glaciology. Whereas most of the studies have focused on the plausibility of using satellite remote sensing for measuring specific glacier parameters or measuring one specific region, there has been a lack of research combining satellite remote sensing and climatic factors to assess the differences in deglaciation among regions. Similarly, due to the recentness of the launch of Landsat 8, there is a shortage of research utilizing the additional bands with the new sensors. The Rocky Mountain and Cascade Ranges are representative of two different geographic and climatic regions. Whereas the Cascade Range is located along the Pacific Ocean and receives high levels of precipitation, the Rocky Mountain Range of the United States is in what is known as the Intermountain Region with a more continental climate. Because of the different climate conditions, the two regions were selected for study. The study was intended to determine the relationship between precipitation rates and the temperature on glacier extents. Glacier areas studied within each region were selected based on availability of images. Glacial calculations for change over time were performed through the implementation of satellite remote sensing and geographic information systems.

OBJECTIVES

The underlying objective of this project was to perform glacial calculations on select glaciers in the Cascade and Rocky Mountain Ranges, utilizing digital remote sensing and geographic information systems, to determine how geographic region and climate influence glaciers. Specifically, the objectives of this study were to:

1. Map and calculate the extent of select glaciers located within the aforementioned areas for the years 1985, 2000, and 2015 to determine possible changes over time.
2. Estimate glacial volume loss over time through the utilization of digital elevation models (DEMs) and satellite imagery.
3. Assess historical weather data and identify trends that would influence the rate of ablation and accumulation for two mountain regions.

LITERATURE REVIEW

Glaciers

A glacier is composed predominantly of perennial ice; it also consists of snow, rocks, various sized sediments, and liquid water which flows within or underneath the glacier itself (USGS, 2019a). According to the U.S. Geological Survey, glaciers form in environments with mean annual temperatures near zero degrees Celsius, where there are high levels of snow accumulation as a result of winter precipitation, or with annual temperatures too low to melt the snow from the former winter season. With time, the snow metamorphoses to glacial ice. As new snow falls, older snow re-crystallizes as a result of compression forces (NSIDC, 2019). Firn is the intermediary phase between compacted snow and glacial ice. The environment in which a glacier forms factors into its size, shape, and classification. This study focuses on alpine glaciers specifically. The minimum area of a glacier is accepted to be 0.1 km^2 (USGS, 2019a). Glaciers are found on the windward side of mountain regions to reflect the locations of greatest snow accumulation (Kuhn, 2010). Glaciers are not stationary but instead they are slowly shifting in position, flowing downslope (Pellikka and Rees, 2010). Glaciers in combination with permafrost, ice sheets, and frozen water bodies make up the cryosphere (Harris and Murton, 2005).

Glacier Systems

Glaciers are systems with inputs and outputs. The mass balance of a glacier is defined by the gaining and loss of ice in the system (Benn and Evans, 2010). Snowfall is the main input to glaciers; other inputs include avalanches and windblown deposits (Kuhn, 2010). The zone in which a glacier grows in response to the inputs is known as the accumulation zone. Outputs are the result of melting, evaporation, or breakage (Benn and Evans, 2010). The area of the glacier that undergoes shrinkage or thinning is collectively referred to as the ablation zone. Most ablation is the result of melting, with the exception of tropical glaciers with high levels of sublimation (Kaser, 2001). The mass balance is the difference between accumulation and ablation. The equilibrium line altitude (ELA) is where the rate of accumulation is equal to the rate of ablation.

Distribution of Glaciers

Glaciers can be found globally. With the exception of Australia, glaciers exist on every continent. Although global trends exist for Earth's glacier dynamics, it is beneficial to assess glacier patterns at a regional scale. The World Glacier Monitoring Service (WGMS) divided the globe's glaciers into 11 macroregions (listed from smallest ice covered area to largest): New Guinea, Africa, New Zealand, Scandinavia, Central Europe, South America, Northern Asia, Antarctica, Central Asia, North America, and Arctic Islands. Some of the macroregions share names with their associated continent; however in several cases, the glacial macroregion is not encompassing of the continent in its entirety, but instead is formed around the area where glaciers are extant. The ice covered area for each of these macroregions is based on glaciers and ice caps and excludes ice sheets. The North American macroregion, with 49,000 km^2 of glaciers in the conterminous United States and Western Canada, was the area of interest for this study (WGMS, 2008).

Influence of Climate

In the context of glaciers, climatic factors that need to be measured include: temperature, radiation, and precipitation (Hall and Fagre, 2003). Most previous studies emphasize either increases in summer temperatures or decreases in winter precipitation. Posamentier (1977) attributed 70% of changes in terminus position to the two variables. Likewise, 73% to 90% of mass balance variations are attributed to deviations in summer temperature and precipitation (Martin, 1974). Based on studies by Braithwaite and Oleson (1989), it was determined that a stronger relationship between cumulative daily totals of degrees above zero temperature and glacier ablation exists than between glacier ablation and mean summer temperature, and although their study focused on glaciers in Greenland, their variable, positive temperature sum, is applicable in methodology to other glacial regions. The temperature of the air varies from the temperature of precipitation (Benn and Evans, 2010). The amount of precipitation an area receives in the form of snow impacts a glacier's near-surface ice temperature; likewise, heat transfer from the air depends on turbulence, which has an impact comparable to wind chill (Benn and Evans, 2010). The humidity of the air and wind speed control evaporation and sublimation; both processes occur due to lower humidity in the air than at a glacier's surface (Benn and Evans, 2010).

The Two Glacier Regions

Intermountain Region: The Rocky Mountain Range

The Rocky Mountain Range extends from Canada in the north to New Mexico in the south, covering a distance of 4,830 km (Marston et al., 1989). Elevation ranges from 1,500 m to 4,400 m (Stohlgren, 1997). Including over 100 smaller ranges, the Rocky Mountains has been divided into four groups: the Canadian Rockies, Northern Rockies, Middle Rockies, and Southern Rockies. The Northern Rockies, the focus of this study, consist of the Clark, Lewis, and Livingston mountain ranges. Within this area, glaciation occurred from the Pleistocene to Holocene Epoch- ending roughly 11,000 years before present; other glaciation events include the Bull Lake Glaciation and Pinedale Glaciation (Stohlgren, 1997). Stohlgren estimated in 1997 that approximately a fourth of the United States' water supply comes from runoff and snowmelt in the Rocky Mountain system.

Glacier National Park

Glacier National Park, as depicted in Figure 1, became a national park in 1910 (NPS, 2009). 1,557 miles of streams are fed by glacial meltwater from within the park (NPS, 2009). In 1850, at the end of the Little Ice Age, what is now known as Glacier National Park had 150 glaciers; when the park was established in 1910, many of these glaciers still existed (USGS, 2019d). Data from 2015 showed a remaining 26 glaciers, with a 73% reduction of glacial area for the park since 1850 (USGS, 2019d; Key et al., 2002). Written records show that deglaciation in the park was observed as early as 1914 as a result of the industrial revolution (USGS, 2019d). From 1910 to 1980, the mean temperature for the summer months increased 1.66° Celsius (Hall and Fagre, 2003).

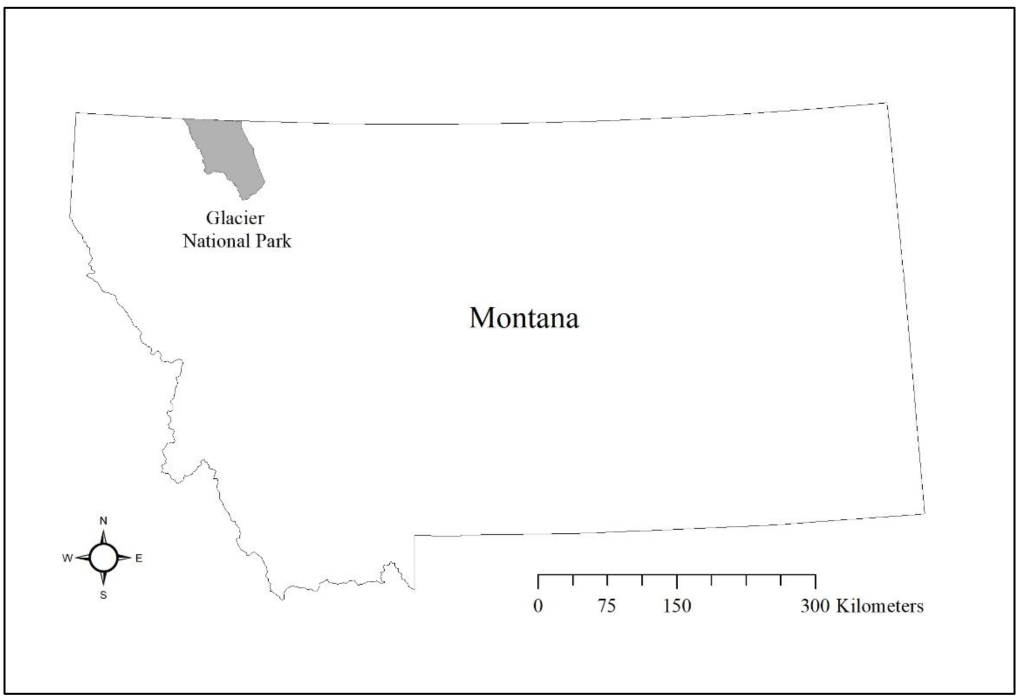

Figure 1. Study area of Glacier National Park in northwestern Montana.

According to a 2017 study by the USGS, all of the park's glaciers have shrunk from their 1966 extents; averaging a loss 39 percent, some glaciers lost as much as 85 percent of their size. Using a glacier simulation software, Hall and Fagre (2003) modeled glacier change within Glacier National Park. They simulated increases in atmospheric carbon dioxide concentrations by 2030 and a 2-3° Celsius increase in temperature by 2050. Based on the simulations, it is predicted that between 2030 and 2080, many of Glacier National Park's remaining glaciers will disappear.

Pacific Northwest Region: The Cascades

The Cascade Range, starting in British Columbia and extending southward over 700 miles to northern California, includes both active and extinct volcanoes; the west side of the range receives an annual average precipitation of 75 cm (USFWS, 2011).

Mount Rainer National Park

Mount Rainer National Park is home to an active volcano by the same name. The elevation of Mt. Rainer is 4,392 m, and the peak has the most glaciers out of all the mountains in the lower forty eight states (NPS, 2017). The national park was established in 1899. The 29 glaciers within the park are well studied. Glacier extent databases from 1896, 1913, 1971, 1994, 2009, and 2015 have already been compiled by the National Parks Service. In 2015, glaciers covered 78.76 km^2 within the park; the same study estimated an average rate of loss of 0.44 km^2 per year for the period of 1896 to 2015 (NPS, 2017). The park has concerns with outburst floods, which is one of the reasons the glaciers are so well studied. The location of Mount Rainier National Park within the state of Washington can be seen in Figure 2.

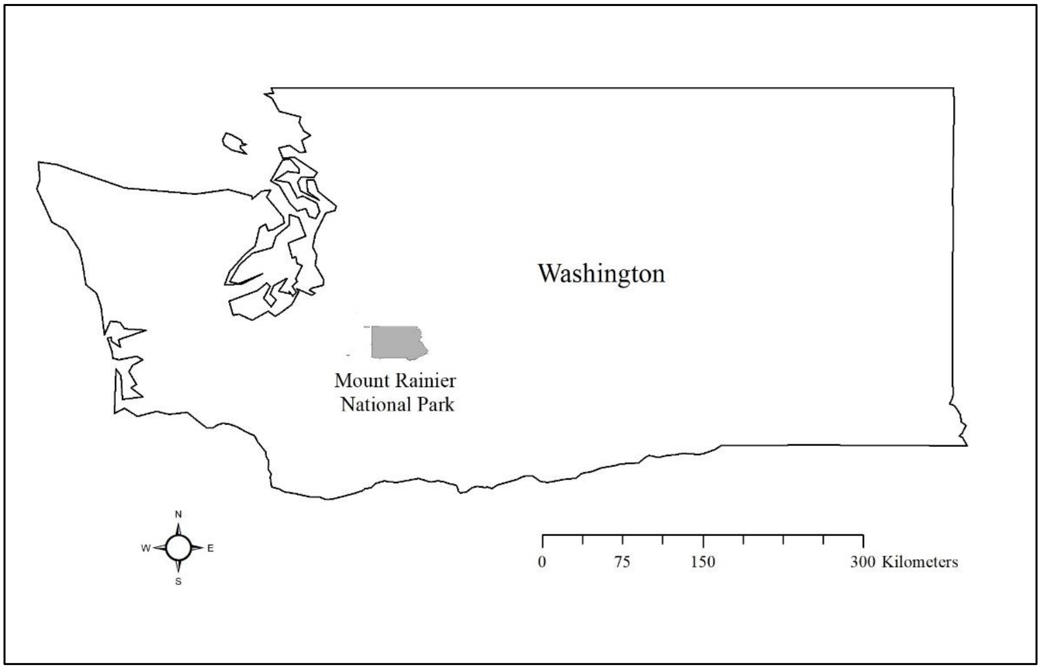

Figure 2. Study area of Mt. Rainier National Park located in southwest Washington.

Digital Remote Sensing

A broad definition of remote sensing is the obtaining of information about the Earth's resources from a distance through the use of electromagnetic energy (Campbell and Wynne, 2011). Often, "from a distance" employs the use of an aircraft or spacecraft/satellite (Richards, 2013). The ability to observe information without direct contact is one of the greatest benefits remote sensing offers. The system of remote sensing begins with the sun emitting energy, energy that then interacts with the Earth's surface and is absorbed, reflected, or transmitted; sensing instruments detect the transmissions and are able to convert the data into image products (Campbell and Wynne, 2011; Richards, 2013). Since the source of the radiation is the sun- a naturally occurring phenomena- passive remote sensing will be utilized.

Background

Starting with the first photograph in 1839, various events throughout history have contributed to the development of modern digital remote sensing; while the field of photography and filmography are interwoven with that of remote sensing, the term "remote sensing" did not originate until 1972 (Campbell and Wynne, 2011). In 1972, the Landsat 1 satellite was launched marking the first satellite devoted to mapping Earth's resources (Campbell and Wynne, 2011). Landsat 1 was part of "Project EROS (Earth Resources Observation Satellites)" launched by the Department of the Interior; the project went on to launch Landsat 2-8 (Landsat 6 never reached orbit) with Landsat 9 scheduled to debut in 2020 (USGS, 2019b). The advantages of Landsat 1 and other satellites of its kind include having a repetitive orbit and the ability to access information on remote locations that are too expensive or dangerous to fly with an airborne platform; the duration of satellite missions' results in data continuity over periods ranging from years to decades (Bossler, 2010; Rees, 2010).

Electromagnetic Spectrum

The electromagnetic (EM) spectrum is the classification of radiation by wavelength or frequency (Rees, 2010). With digital remote sensing, users are concerned with the optical and thermal portions of the electromagnetic spectrum, utilizing the regions inclusive of the visible (0.4-0.7 μm) spectrum and the near (0.7-1.3 μm), mid (1.3-3.0 μm), and far (7.0-15.0 μm) infrared (Richards, 2013; Parcak, 2009). These regions are also referred to as atmospheric windows (Rees, 2010). Spectral bands refer to a range on the electromagnetic spectrum; these bands will vary from satellite to satellite (Richards, 2013; Parcak, 2009). For onscreen display, remote sensing applications allow the user to view a combination of up to three bands concurrently. As to infrared, the near-infrared is useful for vegetation, the mid-infrared for moisture, and the far-infrared for heat (Parcak, 2009). The property of the EM radiation being measured is radiance–intensity of the radiation, which in turn can be converted to an accurate measure of reflectance after undergoing some atmospheric correction (Rees, 2010). Rees (2010) mentions active remote sensing systems that employ the use of ranging instruments and surface reflectance instruments, and although these exist and are applicable to glaciology, they are outside of the scope of this study.

Reflectance

Glaciers can be divided into zones; the typical zones include wet and dry snow, firn, and ice (Pellikka and Rees, 2010). Each zone has a unique reflectance. Impurities on the glacier surface, debris cover, and the presence of frozen lakes impact the reflectance values and spectral signatures (Pellikka and Rees, 2010). Snow is highly reflective in the visible part of the electromagnetic spectrum but has a lower reflectance in the infrareds; firn is 25-30% less reflective than snow, and glacial ice has a high reflectance in the blue and green parts of the spectrum but declines in the red region (Pellikka and Rees, 2010). Since the red light is being absorbed and the blue and green light reflected, glaciers are observed as turquoise (Knap, 1997). Contamination of the snow and ice significantly can lower the reflectance in the visible region, however contaminated ice has a higher reflectance in the near-infrared than clean ice (Hall and Martinec, 1985). Albedo is expressed as a ratio of the radiation reflected compared to the radiation that contacts a surface. Surfaces with higher reflectance have higher albedos. Dry snow has an albedo of 0.80 to 0.97, whereas debris covered ice might have an albedo between 0.15 and 0.25 (Paterson, 1994). Lower albedo values contribute to deglaciation.

Surface Temperature

The top ten meters of a glacier constitute the thermally active surface layer (Pellikka and Rees, 2010). Liquid water on the glacier's surface will be warmer and show an increase in red and near infrared absorption. Factors that lower the albedo also impact surface temperature resulting in faster melting. However once the debris reaches a certain thickness, it can serve as an insulator. Surface temperature of the glacier is lower than that of the surrounding landscape, so the thermal infrared band can be utilized to create a glacier outline (Pellikka and Rees, 2010). A previous study tested methods of creating glacier masks with Landsat ETM+ data, comparing the thermal infrared band (TM6) to band ratios of TM3/TM5 and TM4/TM5 and the NDSI (normalized difference snow index); the study found the thermal band to be the most effective (Heiskanen, 2002).

Image Resolution

The resolution of an image is a measure of the degree of detail displayed; remote sensing systems are concerned with spatial, spectral, radiometric, and temporal resolutions (Campbell and Wynne, 2011). The resolution determines the distinguishability of an object, and the resolution of a satellite determines its resourcefulness for differing applications (Rees, 2010). Spatial resolution correlates to pixel size with finer spatial resolution allowing higher level of detail (Rees, 2010). Spectral resolution relates to a satellite's bands and the extent of the electromagnetic spectrum represented (Campbell and Wynne, 2011). Radiometric resolution is a measure of the number of intervals brightness or radiance can be recorded; 8-bit data is represented with digital numbers between 0 and 255 (Rees, 2010). Temporal resolution relates to the interval of time between the collections of datasets depicting the same location.

Temporal Resolution for Glacier Monitoring

Different characteristics of glaciers are observed at varying temporal resolutions. Geodetic mass balances, terminus positions, and equilibrium line altitudes of glaciers should be calculated at the end of the ablation season, which occurs late into the summer; during this time period, the surface of the ice is at the yearly high for snow-free exposure (NPS, 2009). The end of the glacier's year varies by latitude. Wastlhuber et al. (2017) chose images from the start of August through mid-September for their study. When using satellite images from previous years, a record of that year's precipitation should be consulted to avoid using imagery from a year that experienced late-season snow (NPS, 2019; Riedel and Burrows, 2005). The intervals between the images depends on the size of the glacier and its main source of accumulation (i.e., precipitation versus avalanches). Availability of cloud free data is usually one of the most critical factors as to which images are acceptable for study, despite their temporal resolution.

Landsat Satellites

Data from three Landsat satellites were used in the mapping of glaciers for the extent of this thesis: Landsat Thematic Mapper (TM), Enhanced Thematic Mapper (ETM+), and Landsat Operation Land Imager (OLI) and Thermal Infrared Sensor (TIRS); from Landsat 5 (1984), 7 (1999), and 8 (2013) respectively. Landsat 5 and 7 have seven bands at 30 m resolution that cover from 0.45-1.75, 2.08-2.35, and 10.40-12.50 micrometers; Landsat 7 has an additional panchromatic eighth band that covers wavelengths 0.52-0.90 micrometers at a 15 m resolution (USGS, 2019c). Landsat 8 has supplementary bands for ultra-blue, cirrus, and thermal. Table 1 presents the detailed wavelength for each band and its spatial resolution from the aforementioned sensors.

Landsat satellites can be used to map glaciers greater than 0.02 km^2 (Paul et al., 2003). TM band 1 (TM1) before being atmospherically corrected enables the user to identify snow and ice in shadows (Paul et al., 2005). With TM1, there is a high contrast between contaminated and clean ice, and the sensor assists in reducing saturation (Paul and Hendriks, 2010). TM2 similarly allows for identification of features in shadows, but it also classifies water bodies; TM3 and 4 aid in vegetation classification and are used in the normalized difference vegetation index (Paul and Hendriks, 2010). Snow has a lower reflectance in the near infrared (NIR) band TM4 than in bands TM2 or 3 (Paul and Hendriks, 2010). TM5 and 7 can be used to identify ice from snow because ice will have lower digital numbers; it also helps to identify clouds (Paul and Hendriks, 2010). TM6 assists in determining the depth of debris cover (Mihalcea et al., 2008). Although these descriptions are specific to Landsat TM bands, the same measurements can be performed using the corresponding bands on the other two satellites.

Table 1. Description of individual bands for Landsat 5, 7, and 8 based on information obtained from *GIS Geography* (2019).

Landsat 5 Thematic Mapper			
Band Number	Description	Wavelength (µm)	Resolution (m)
Band 1	Visible Blue	0.45-0.52	30
Band 2	Visible Green	0.52-0.60	30
Band 3	Visible Red	0.63-0.69	30
Band 4	Near-infrared	0.76-0.90	30
Band 5	Short-wave infrared	1.55-1.75	30
Band 6	Thermal	10.4-12.3	120
Band 7	Short-wave infrared	2.08-2.35	30
Landsat 7 Enhanced Thematic Mapper			
Band 1	Visible Blue	0.45-0.52	30
Band 2	Visible Green	0.52-0.60	30
Band 3	Visible Red	0.63-0.69	30
Band 4	Near-infrared	0.76-0.90	30
Band 5	Mid-infrared	1.55-1.75	30
Band 6	Thermal	10.4-12.3	60
Band 7	Mid-infrared	2.08-2.35	30
Band 8	Panchromatic	0.52-0.90	15
Landsat 8 Operational Land Imager and Thermal Infrared Sensor			
Band 1	Coastal/Aerosol	0.4333-0.453	30
Band 2	Visible Blue	0.450-0.515	30
Band 3	Visible Green	0.525-0.600	30
Band 4	Visible Red	0.630-0.680	30
Band 5	Near-infrared	0.845-0.885	30
Band 6	Short Wavelength infrared	1.56-1.66	30
Band 7	Short Wavelength infrared	2.10-2.30	60
Band 8	Panchromatic	0.50-0.68	15
Band 9	Cirrus	1.36-1.39	30
Band 10	Long Wavelength infrared	10.3-11.3	100
Band 11	Long Wavelength infrared	11.5-12.5	100

Digital Elevation Models (DEMs)

In order to calculate volume or mass balances, DEMs and glacier outlines are necessary (Racoviteanu et al., 2008). In February 2000, the Shuttle Radar Topography Mission (SRTM) resulted in a global dataset of elevation data; however due to slope induced errors, SRTM data is inaccurate for calculations regarding alpine glaciers (Racoviteanu et al., 2008). Additionally, since it was flown in February, the data taken coincided with the accumulation season for specific latitudes (Racoviteanu et al., 2008). Instead, ASTER-derived DEMs with ground control points (GCPs) from topographic maps or satellite images were used for this study. Additional DEMs will need to be erected from historic topographic information, in order to estimate changes in elevation over time (Racoviteanu et al., 2008).

Parameters

The following parameters were selected based upon the study's objectives. The following review focuses more on the methods used in the literature than the results produced. Results for glaciers not within the study area were deemed irrelevant.

Area

Methods for calculating glacier area include manual delineation of perimeters, band ratio techniques, supervised/unsupervised classifications, and object-oriented classification (Pellikka and Rees, 2010). Wastlhuber et al. (2017) used GIS to extract glacier outlines from topographic maps in digital raster graphic format; the Randolph glacier inventory provides outlines of the glaciers for more recent years. The most common threshold ratios used include TM3/TM5, TM4/TM5, and the normalized difference snow index (NDSI): (TM2-TM5)/(TM2+TM5). Atmospherically correcting the digital numbers aids in the spectral separation and eliminates some of the effects of shadow (Crippen, 1988). Crippen (1988) compared various band ratioing techniques and found that the NDSI was the most accurate. After applying the NDSI, the image will have values ranging from -1 to 1; a threshold value is then used to make a binary map of glacier areas (Racoviteanu et al., 2008). Values greater than the threshold are considered snow and ice; previous studies have used thresholds of 0.4, and 0.5-0.6 (Racoviteanu et al., 2008). Threshold values will vary by scene and are adjusted based on the albedo values of the snow and ice. Clouds can be separated from ice and snow through using a false color composite using TM5, TM4, and TM3 (Hendriks and Pellikka, 2007). Debris covered ice is often included in the glacier outlines; manual adjustments can be made based on thermal differences between the ice and debris (Kienholz et al., 2015).

Volume

Wastlhuber et al. (2017) utilized DEMs constructed by the USGS and ASTER DEMs to calculate elevation changes; the datasets were projected to the same datum and geometrically corrected and co-registered to account for the unavailability of reliable ground control points in the older datasets. The change in elevation (Δz) is equal to the elevation at the time of the older DEM (t_2) minus the elevation of the initial DEM (t_1)

(Pellikka and Rees, 2010). Wastlhuber et al. (2017) used the calculated elevations and multiplied them by the area of the glaciers to find volume, and using an assumed constant density of 850 kg m^{-3}, determined mass changes. The density of 850 kg m^{-3} is lower than the density of ice; the inconsistency attempts to accurately represent firn layers of a lower density (Wastlhuber et al, 2017). This methodology is consistent with the methods by Racoviteanu et al. (2008).

METHODS

Data Acquisition

Image Acquisition

Images for the study were from Landsat satellites 5, 7, and 8. The Landsat 5 and 7 images were obtained freely from the USGS Earth Explorer website (http://earthexplorer.usgs.gov), already orthorectified (USGS, 2019e). However the Landsat 8 scenes available for immediate download were not previously atmospherically corrected, so Level 2 data was ordered. Level 2 data includes bands 1 through 7 atmospherically corrected. These bands were then stacked with Level 1 bands to create the full 11 band Landsat 8 scene. The dates selected for the images correspond with the end of the ablation season, but were ultimately dictated by the availability of images without cloud cover obscuring the glaciers (Table 2). Images were selected for the years 1985, 2000, and 2015 (Figures 3-8).

Table 2. Landsat scenes used for both study areas.

Landsat Satellite	Date	Path/Row
5	19-Jul-85	41/26
5	23-Aug-85	46/27
7	25-Sep-00	46/27
7	8-Oct-00	41/26
8	23-Aug-15	41/26
8	27-Sep-15	46/27

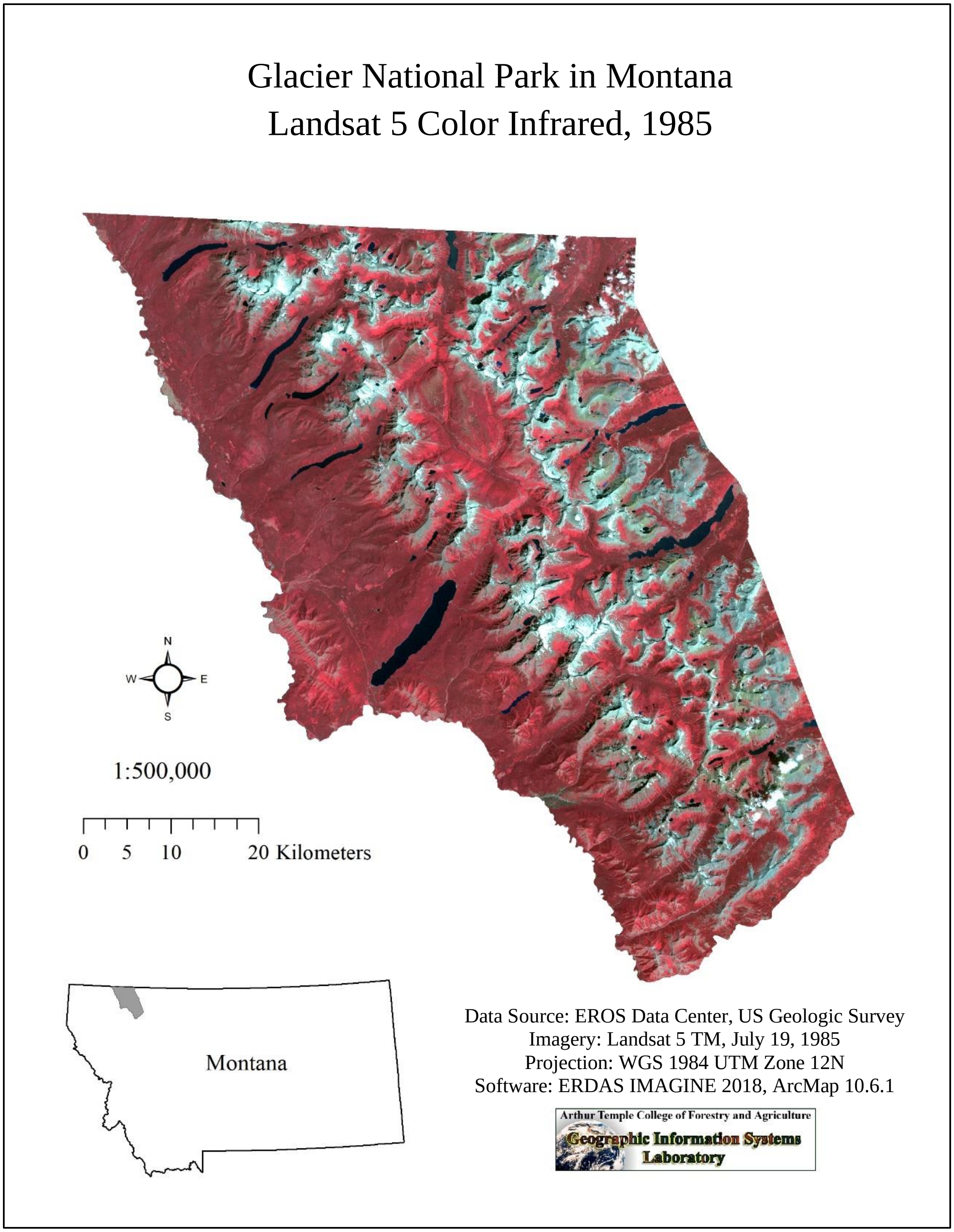

Figure 3. CIR image of Glacier National Park July 19, 1985.

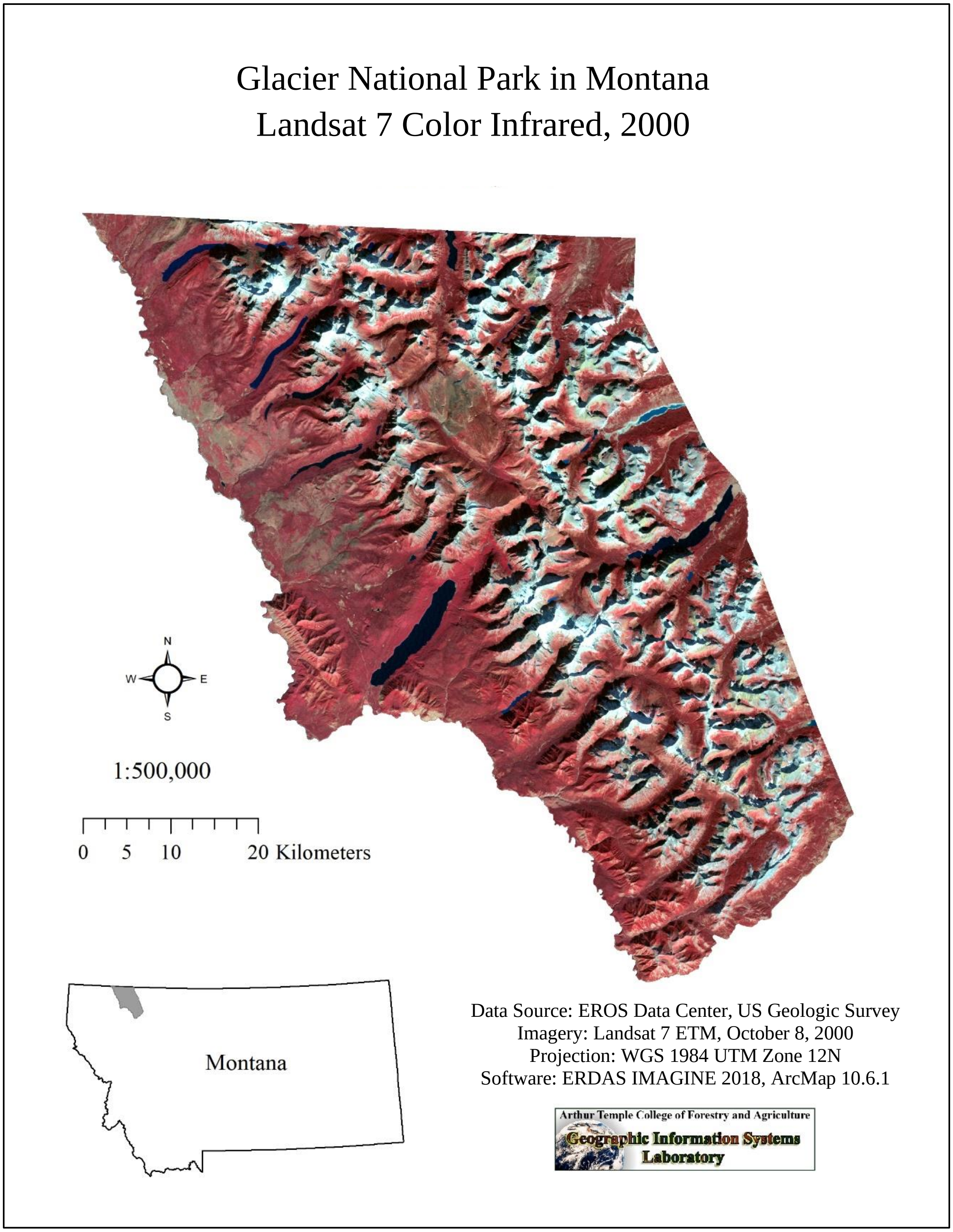

Figure 4. CIR image of Glacier National Park October 8, 2000.

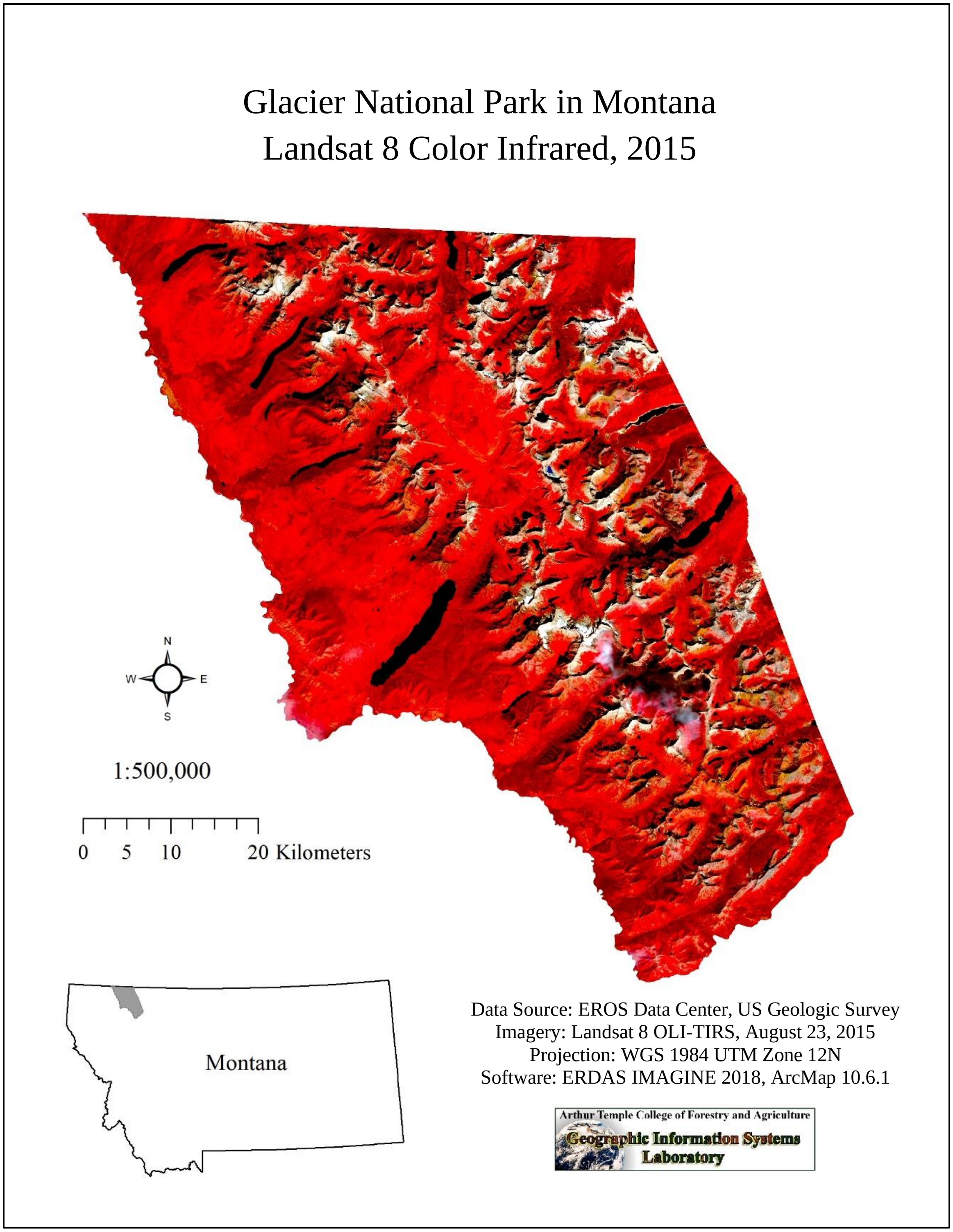

Figure 5. CIR image of Glacier National Park August 23, 2015.

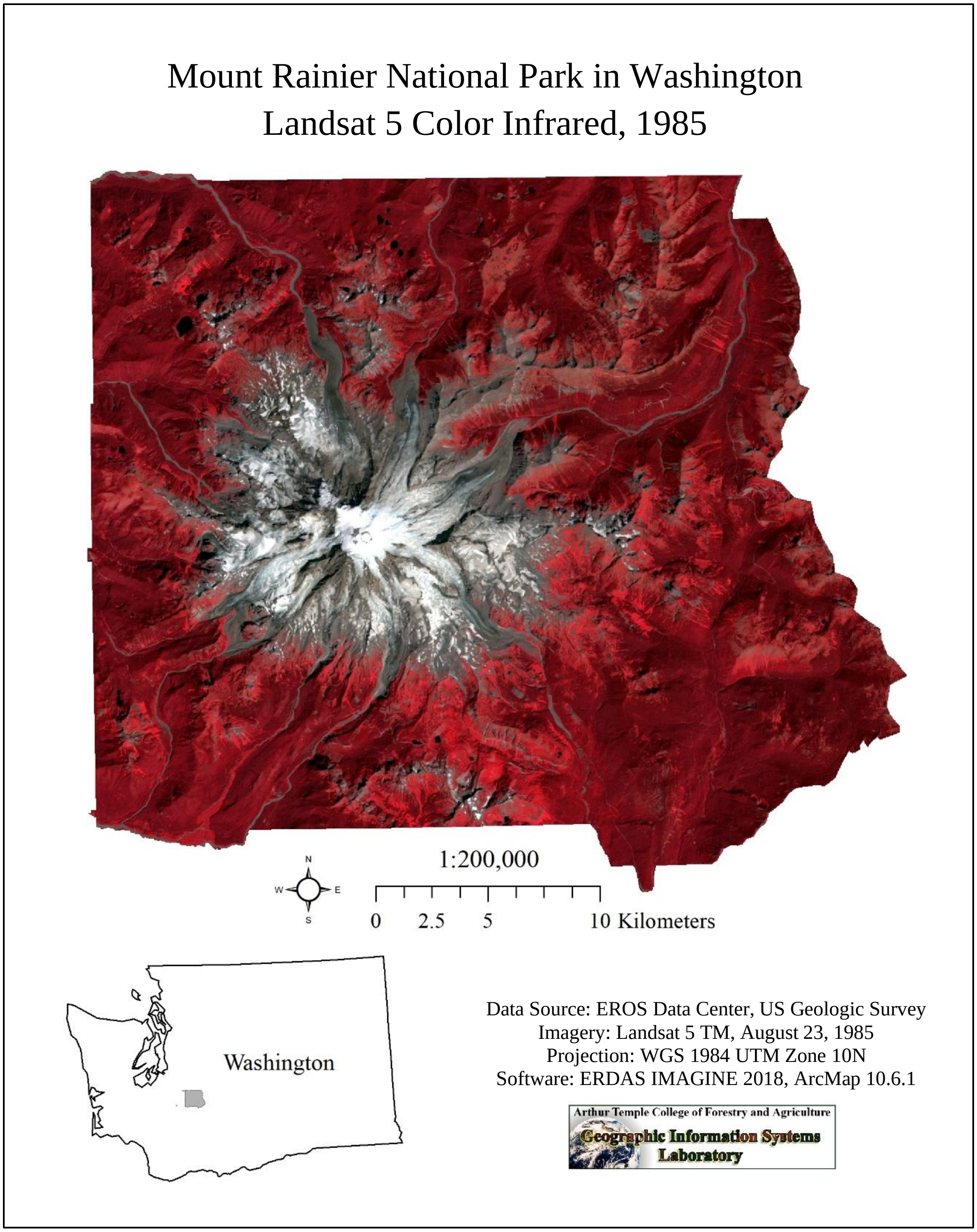

Figure 6. CIR image of Mount Rainier National Park August 23, 1985.

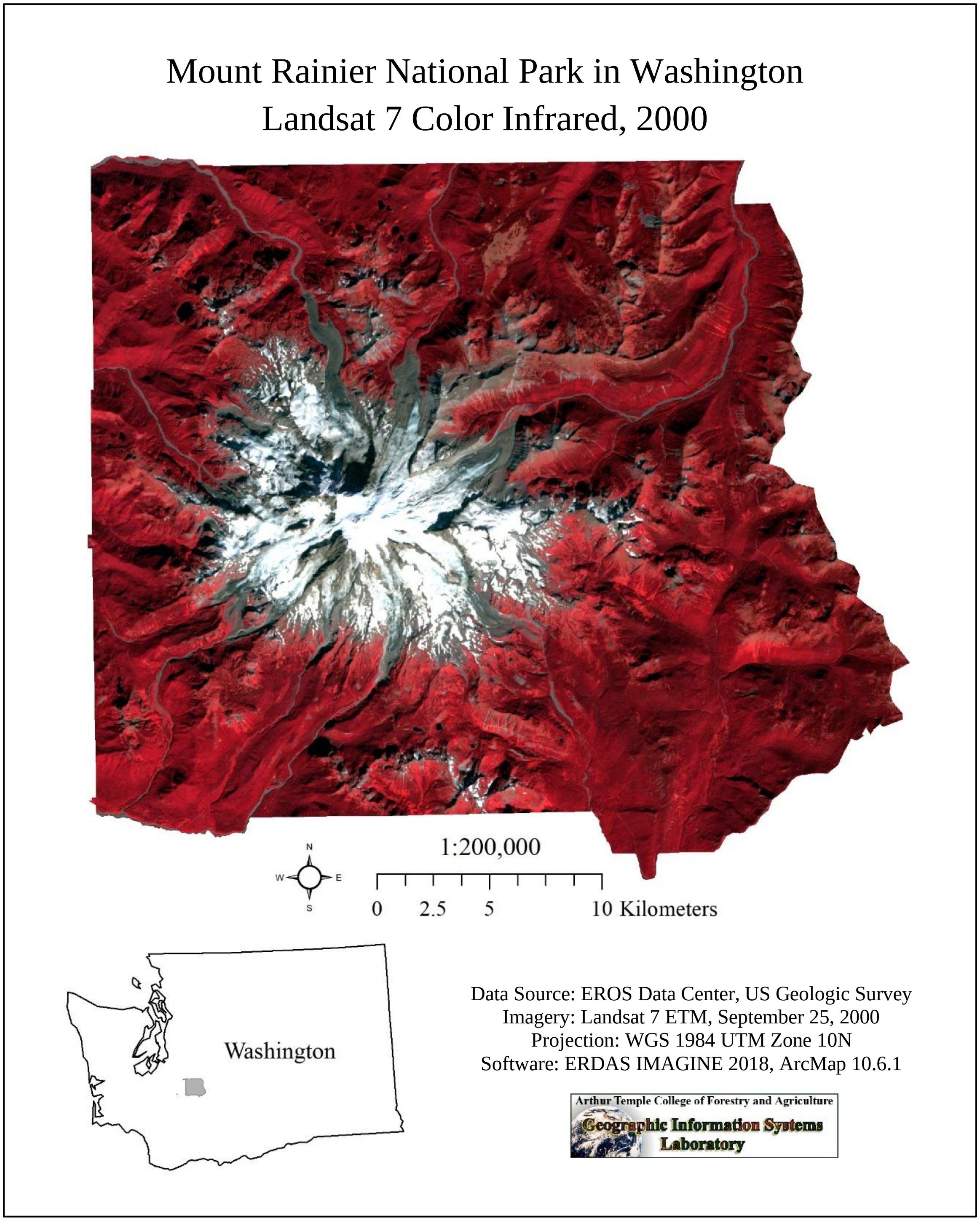

Figure 7. CIR image of Mount Rainier National Park September 25, 2000.

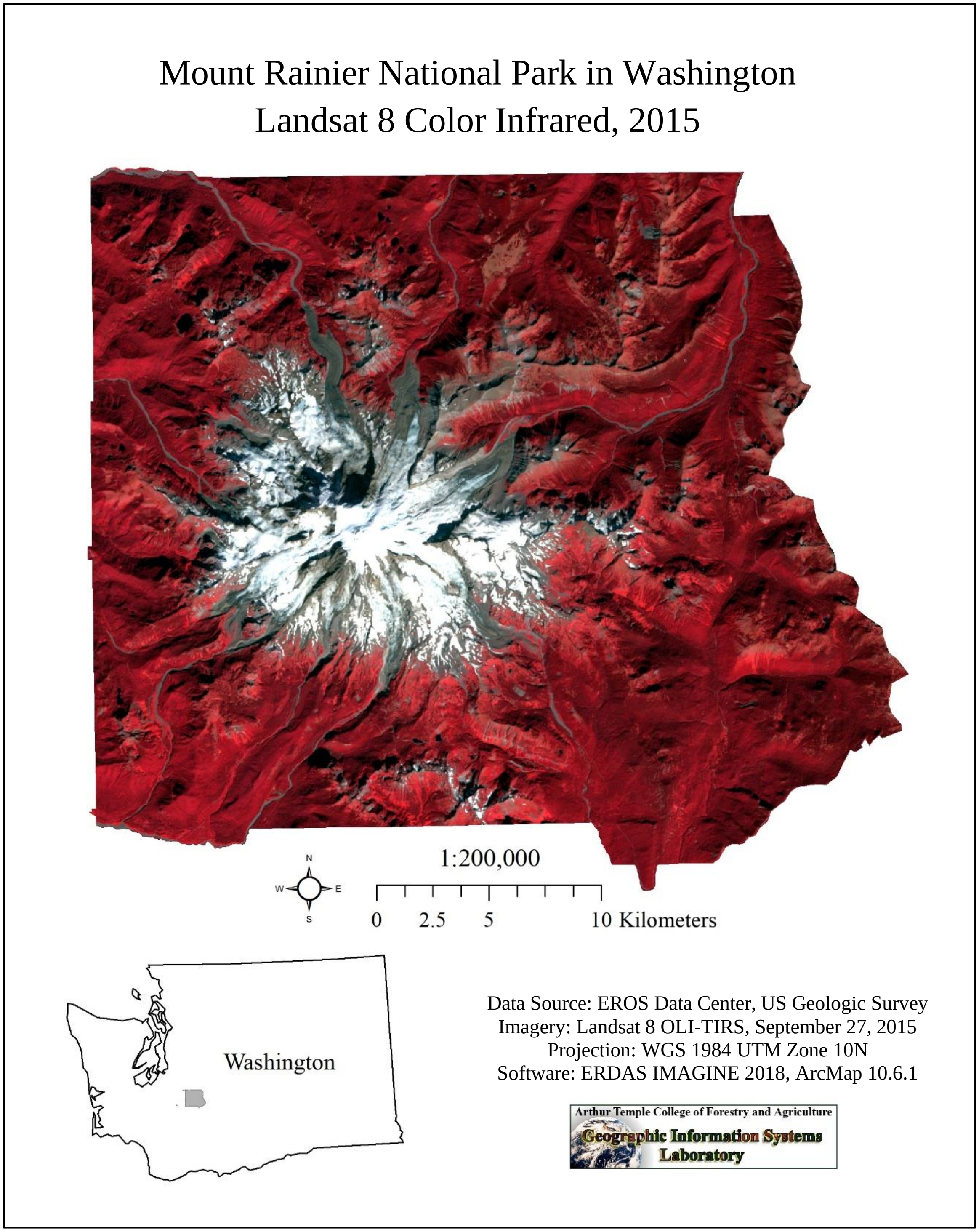

Figure 8. CIR image of Mount Rainier National Park September 27, 2015.

Digital Elevation Model (DEM) Acquisition

Digital Elevation Models were not available for the years 1985 and 2015, so DEMs were created through the digitization of historical topographic maps and the download of contour lines. Contour lines were downloaded from USGS The National Map (http://viewer.nationalmap.gov/basic) (Table 3) (USGS, 2020a), representing the terrain of 2015. Historical topographic maps were downloaded from USGS TopoView (http://ngmdb.usgs.gov/topoview/viewer) in the form of a georeferenced tiff file (Table 4) (USGS, 2020b) that depicted the terrain of 1985. Contour lines and topographic maps were not available specifically for 1985 and 2015, so the closest available years were used. These contour lines and topographic maps do not represent a specific time of year because they were developed over months to years. The historical topographic maps were projected to the relevant datum: WGS 1984 UTM Zone 10N for Mt. Rainier National Park and Zone 12N for Glacier National Park. The contour lines in the topographic maps were digitized into a polyline shapefile and the Topo to Raster interpolation tool in ArcMap was utilized to create DEMs from the lines. Since only contours of glacial terrain were needed, a 500 meter buffer was created around the 1985 glacier extents to ensure that the same size area was compared for each year, and only the contour lines within the buffer were digitized.

Table 3. Contour line files downloaded from USGS The National Map and the dates the files were created.

Date	Contour Details
12/2010 - 06/2013	USGS NED 1/3 arc-second contours for Yakima W, Washington
02/2011 - 07/2011	USGS NED 1/3 arc-second contours for Cut Bank W, Montana
02/2011 - 01/2014	USGS NED 1/3 arc-second contours for Kalispell E, Montana

Table 4. 1:100,000 scale metric topographic maps.

Date	Topographic Map Details
1978	Mount Rainier, WA
1981	Saint Mary, MT
1981	Whitefish Range, MT
1981	Hungry Horse Reservoir, MT

Glacier Extents

Due to the amount of interest in the glaciers of North America, glacier extents were available for download through the Northern Rocky Mountain Science Center (https://www.sciencebase.gov/catalog/item/58af7022e4b01ccd54f9f542?community=Northern+Rocky+Mountain+Science+Center) for Glacier National Park for the years 1966, 1998, and 2015 (Fagre et al., 2017). These downloads were formatted as ESRI Shapefiles. The downloaded boundaries were only used as a reference. Glacier boundaries for all the years of the study were derived through applying the NDSI index and ratioing techniques.

Weather Data

Weather data was downloaded from the National Oceanic and Atmospheric Administration (https://www.ncdc.noaa.gov/cdo-web/datasets) for daily minimum and maximum temperature values and snowfall (NOAA, 2020). Only one station was located in Mount Rainier National Park; however, multiple stations exist within Glacier National Park (Table 5). The Many Glacier station had the most centralized location within the park and was closest in elevation to the station at Mount Rainier, so it was used for comparing temperatures. The Many Glacier station did not record snowfall, so the East Glacier station was used for snowfall. Weather data for 1985 was not available for the Many Glacier station, but existed for the remaining 29 years being measured.

Table 5. Weather stations being utilized to analyze climate trends.

Station ID	Station Name
GHCND: USC00456898	Rainier Paradise Ranger Station, WA US
GHCND: USC00242629	East Glacier, MT US
GHCND: USS0013A27S	Many Glacier, MT US

Data Processing

Area Calculations

A shapefile that contained all of the national park boundaries was downloaded (http://catalog.data.gov/dataset/national-parks) (NPS, 2019). Layers were created from the selected features for Glacier National Park and Mount Rainier National Park, and the data was then exported and saved as individual shapefiles. In ArcToolbox, the Extract by Mask tool was used to subset each Landsat scene to the boundary of the national parks. For this tool to be available, the Spatial Analyst extension had to be enabled. The output raster was then used as the input for the Normalized Difference Snow Index (NDSI) [VIS-MIR] / [VIS+MIR] in ERDAS IMAGINE. A model was built to apply a threshold of $\geq$ 0.7 for Glacier National Park and $\geq$ 0.4 for Mount Rainier National Park (Figure 9). The threshold value was selected based on a visual inspection of the results and known glacier areas and held constant for the study area for all three images. Using the threshold value, a binary map was created denoting ice from non-ice. The Normalized Difference Glacier Index (NDGI) [Green-Red] / [Green+Red] was also used for Mount Rainier National Park due to the amount of glacier area covered by debris. The threshold value used was $\leq$ 0. This process is depicted in Figure 10. Figures 11 through 16 contain the outputs from the NDSI; Figures 17 through 19 portray the NDGI outputs. In order to manually adjust the vertices, the files needed to be modified to be more compatible in ArcMap. In ArcMap, the pixels were reclassified using the Reclassify tool. "0" should be "NoData", "1" should stay "1", all other numbers should be removed, and "NoData" should be "NoData". The reclassified file was then converted to a vector file using the conversion tool, Raster to Polygon. In order to delete misclassified pixels, a new field for area was created in the attribute table of the new shapefile. The new field's type was float, precision: 20, and scale: 10. These parameters were based on methods presented by Bolch, 2013. The field's geometry was then calculated and attributes with areas less than

0.05 km^2 were selected and deleted. (The editor toolbar must be enabled). The vertices of the NDSI shapefiles were then manually manipulated to account for the debris cover highlighted by the NDGI and the underlying satellite image. The geometry was then recalculated in the attribute table, and the total area calculated in the table's statistics.

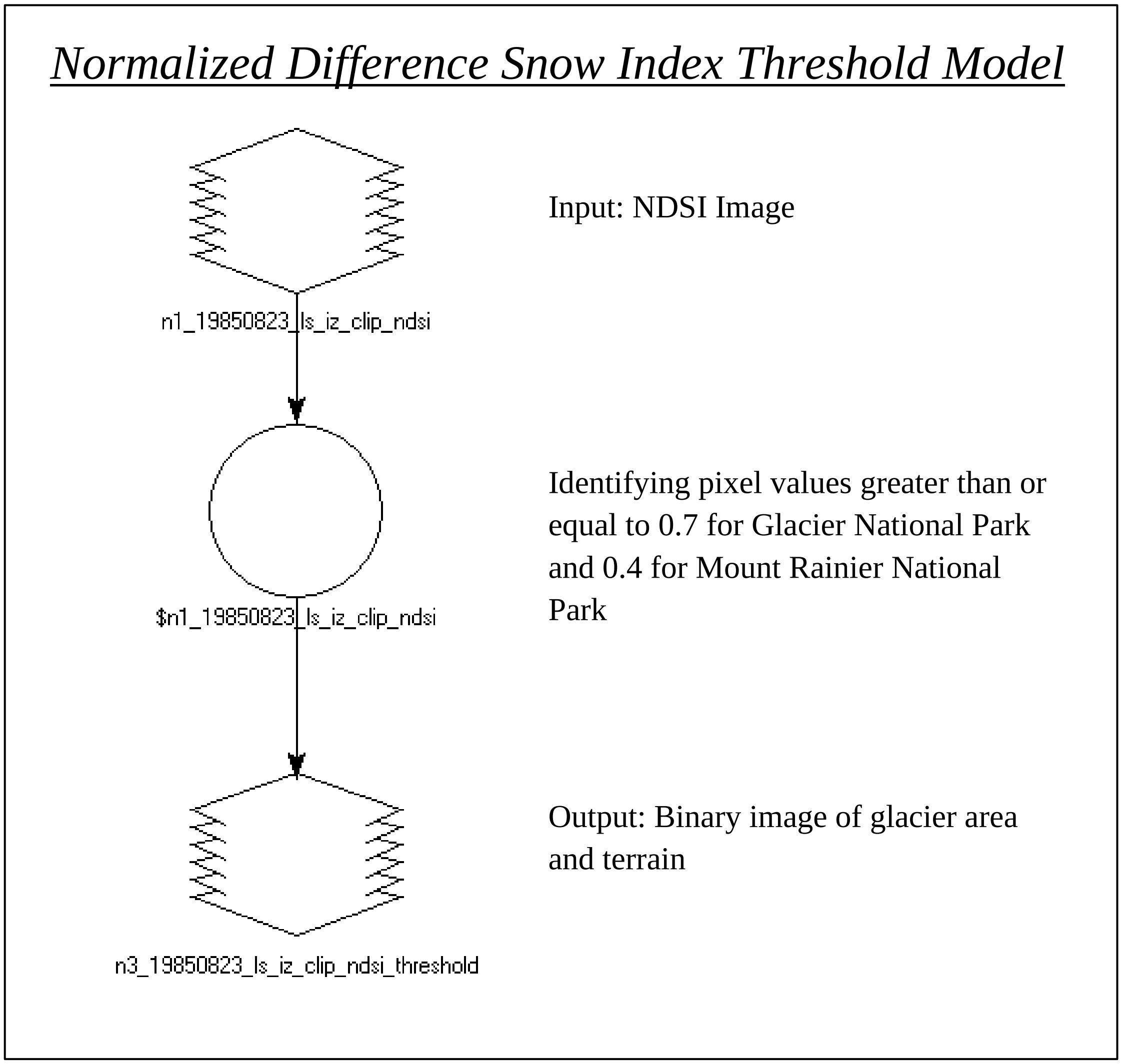

Figure 9. An example of the models used to create binary images from the NDSI and NDGI outputs.

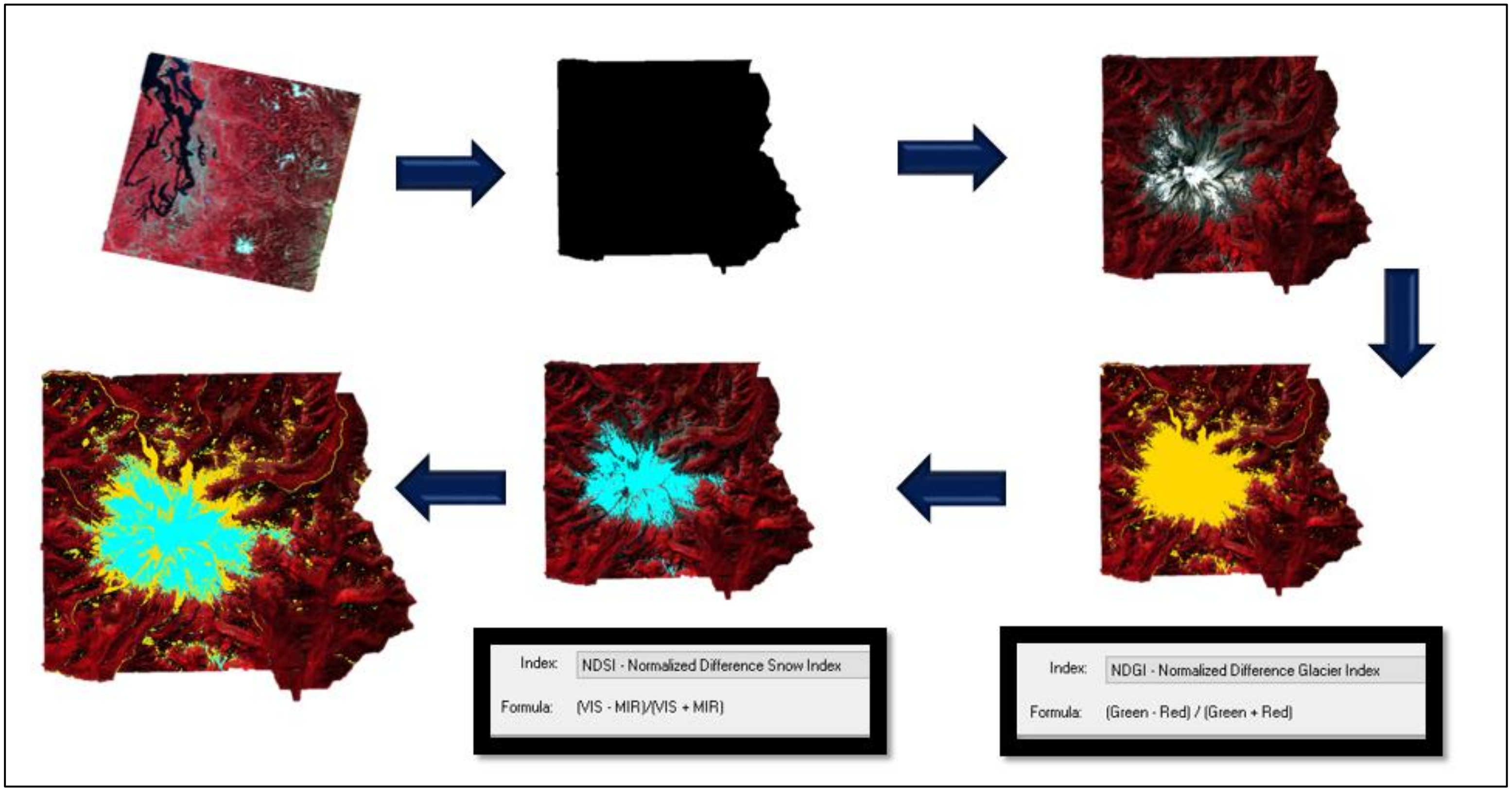

Figure 10. Graphic visualization of the process of applying the extract by mask tool and band ratio techniques.

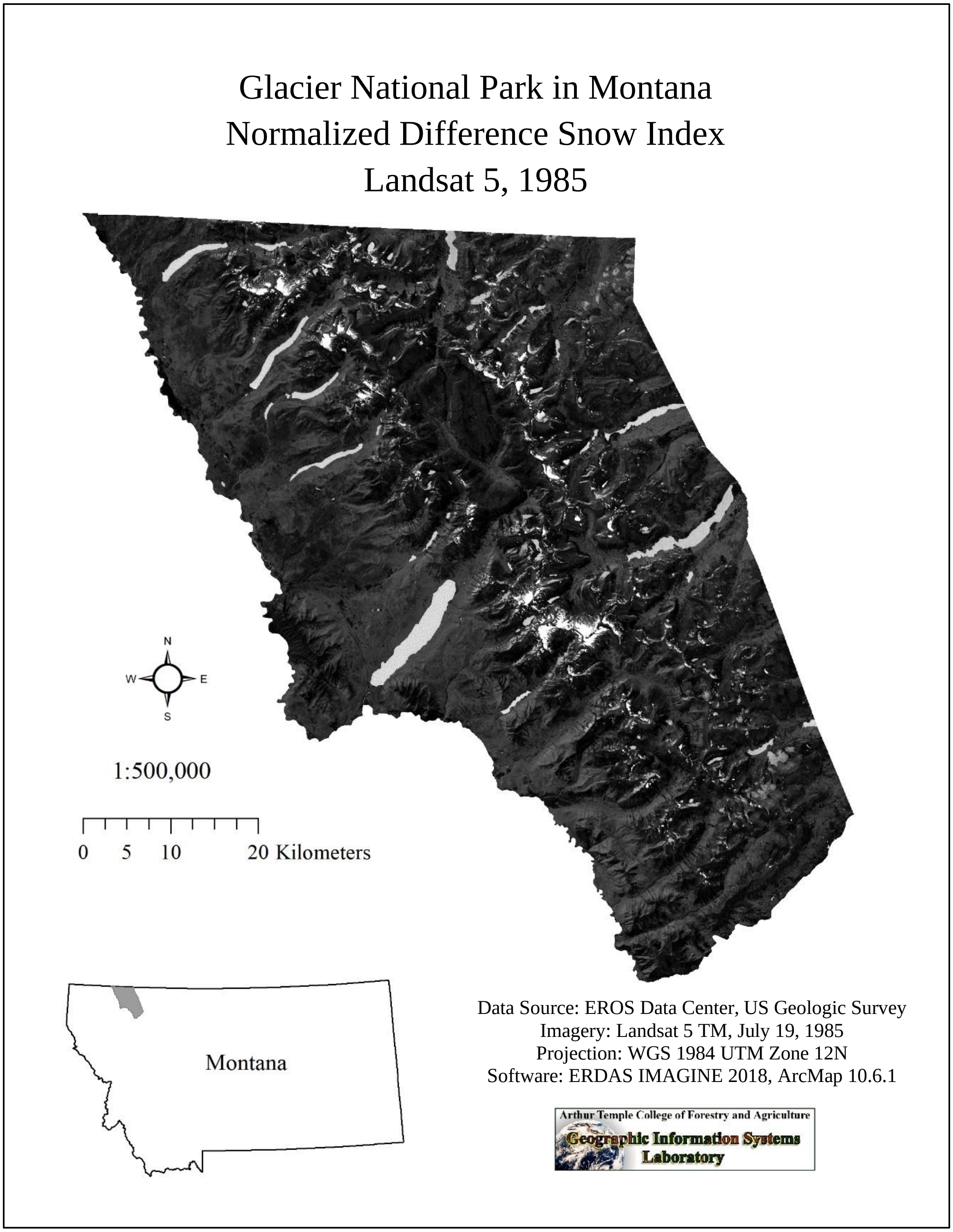

Figure 11. NDSI for Glacier National Park in 1985.

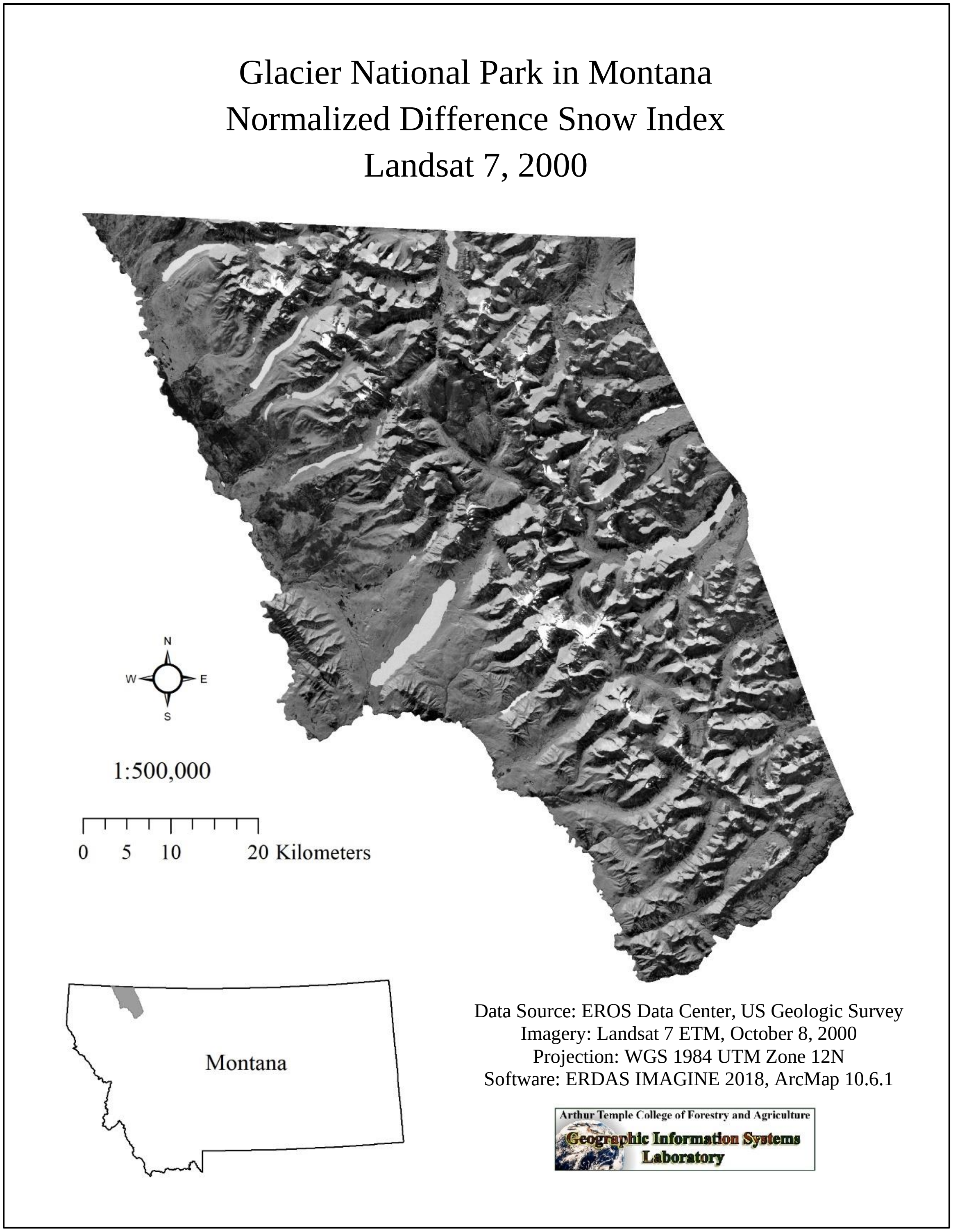

Figure 12. NDSI for Glacier National Park in 2000.

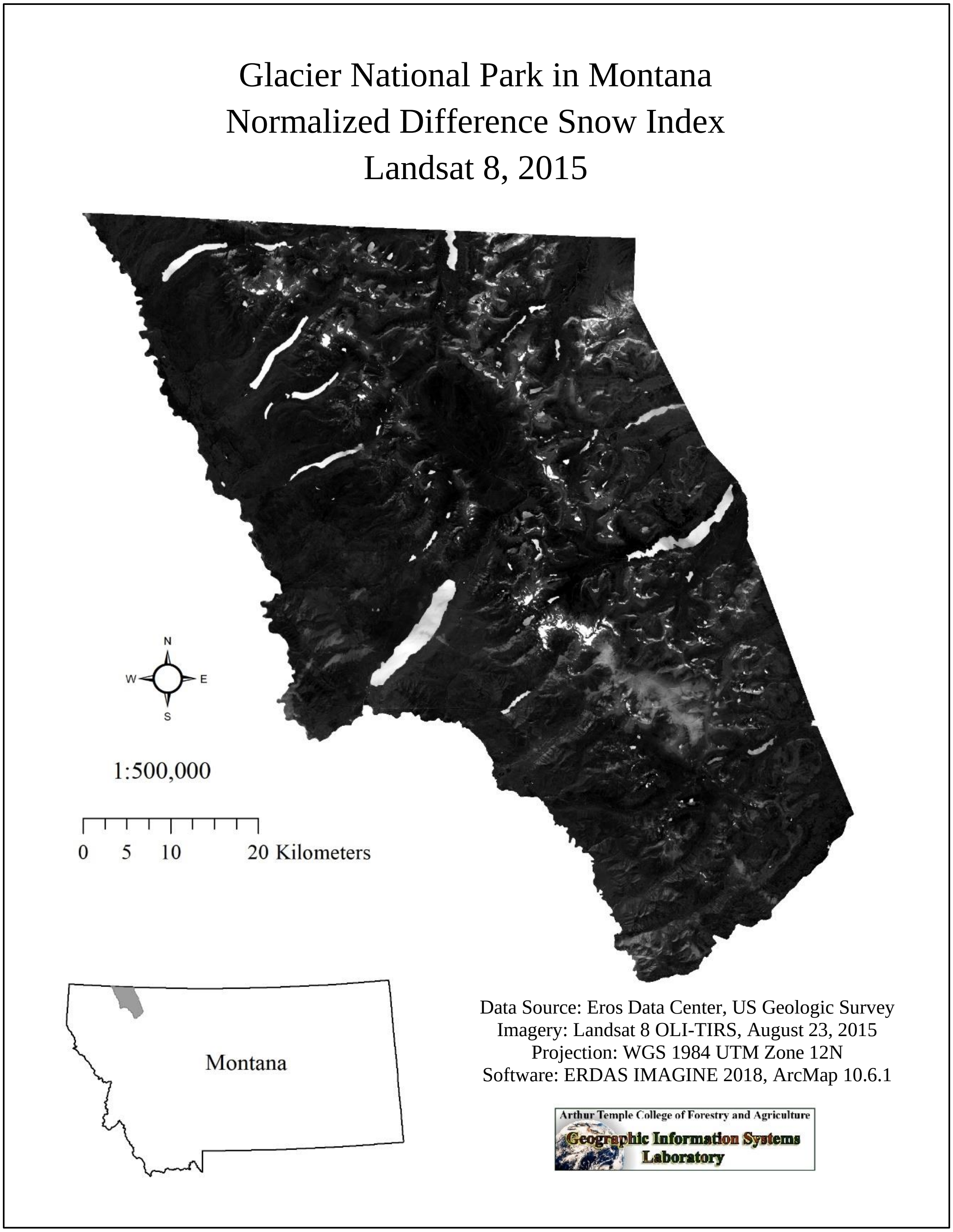

Figure 13. NDSI for Glacier National Park in 2015.

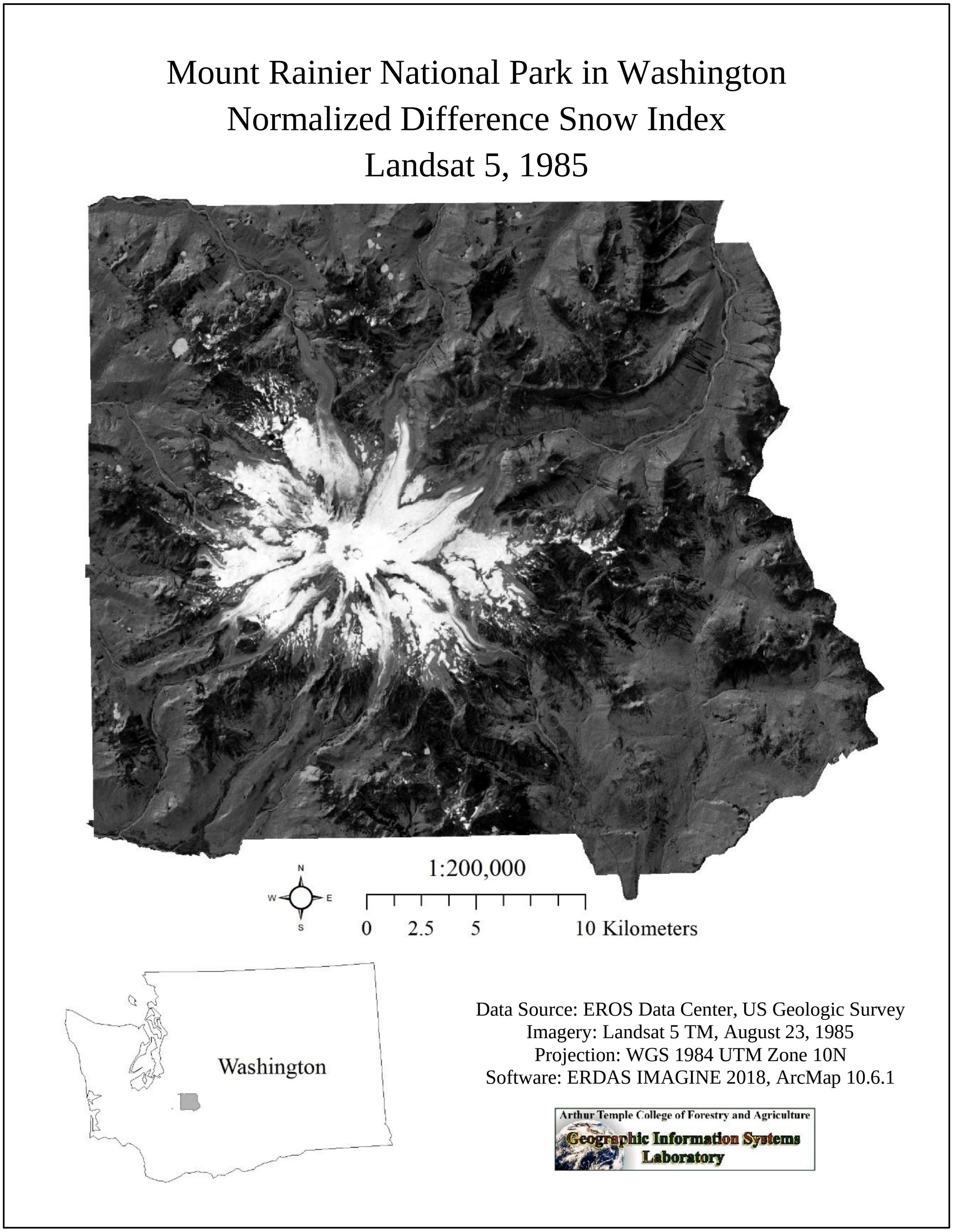

Figure 14. NDSI for Mount Rainier National Park in 1985.

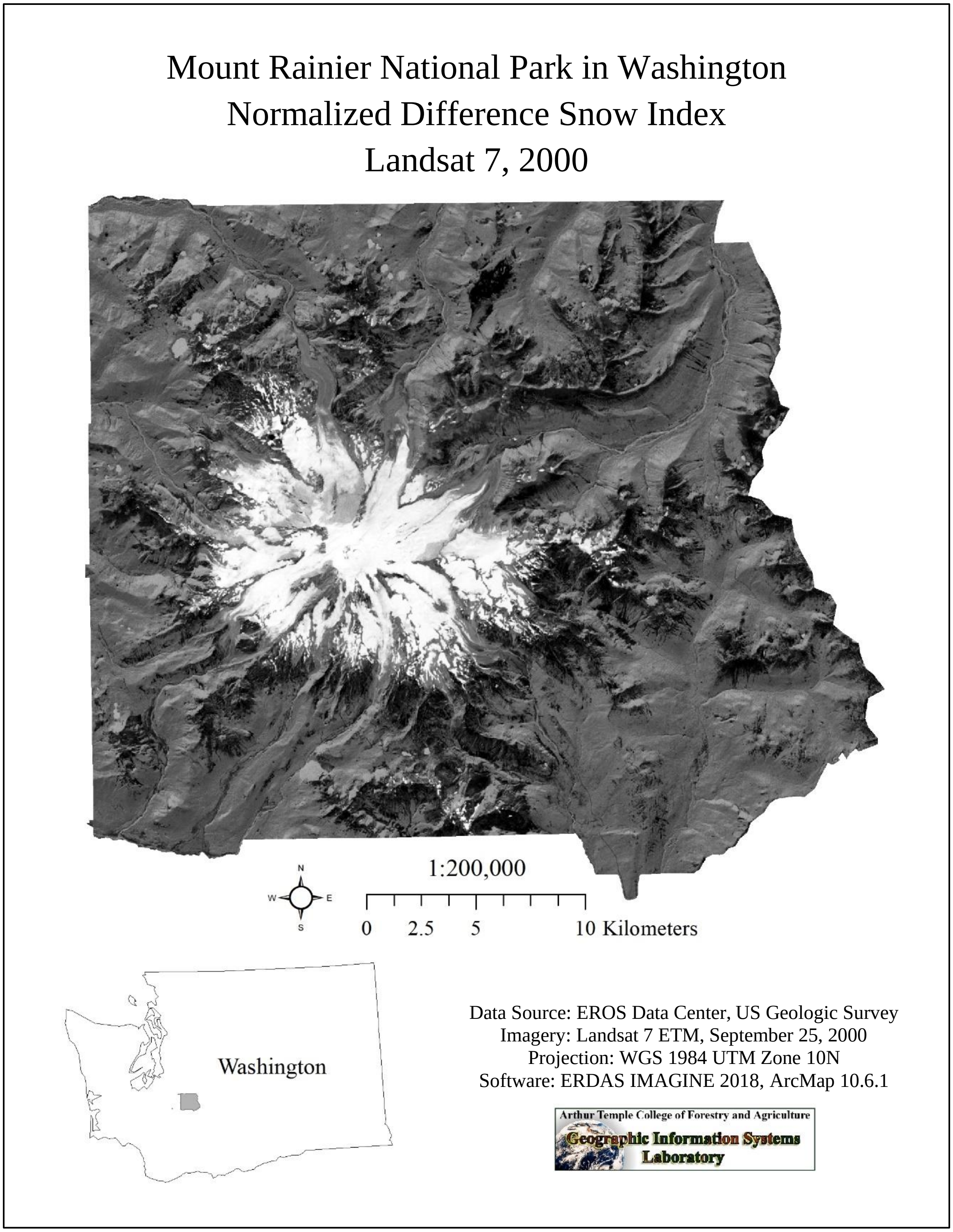

Figure 15. NDSI for Mount Rainier National Park in 2000.

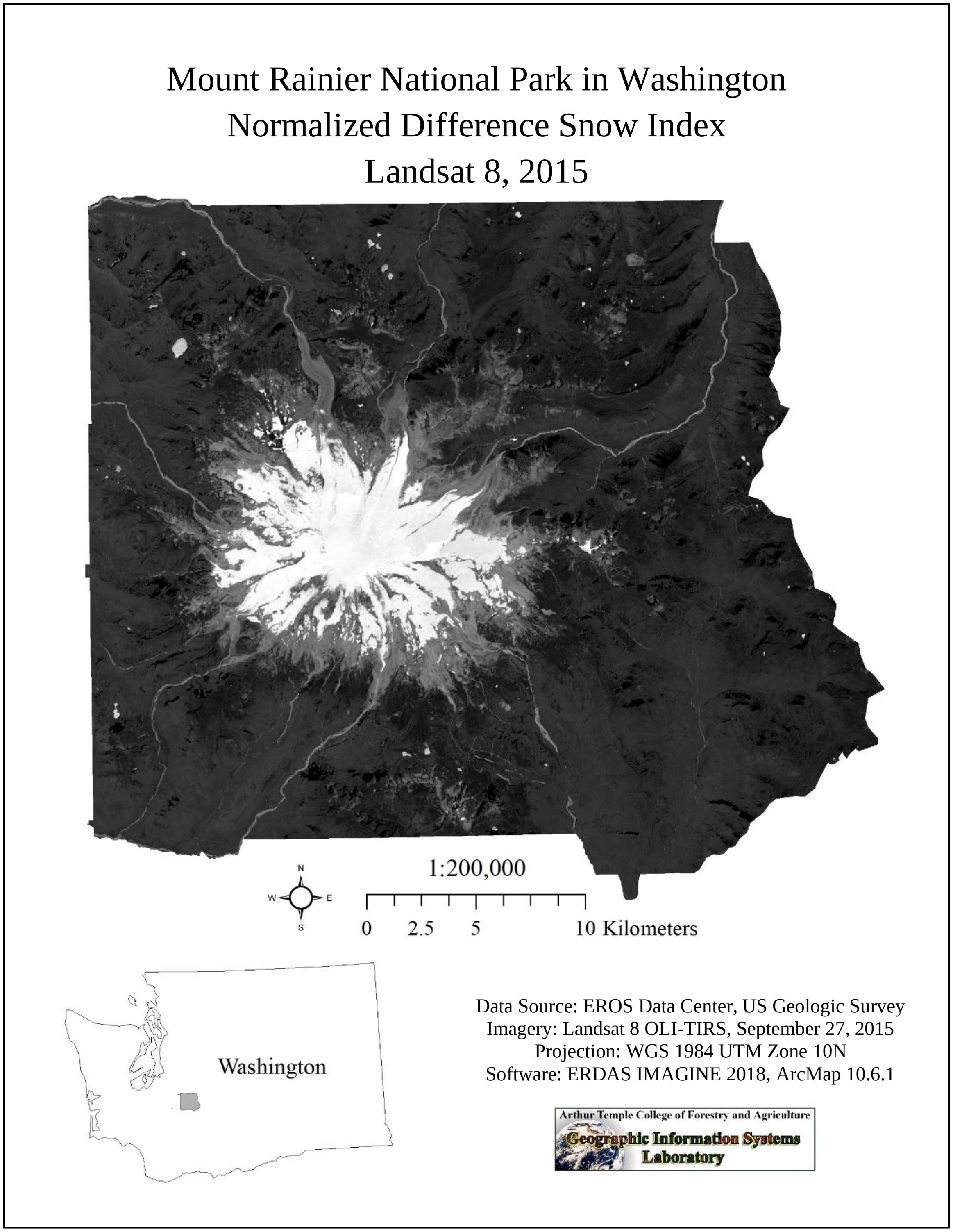

Figure 16. NDSI for Mount Rainier National Park in 2015.

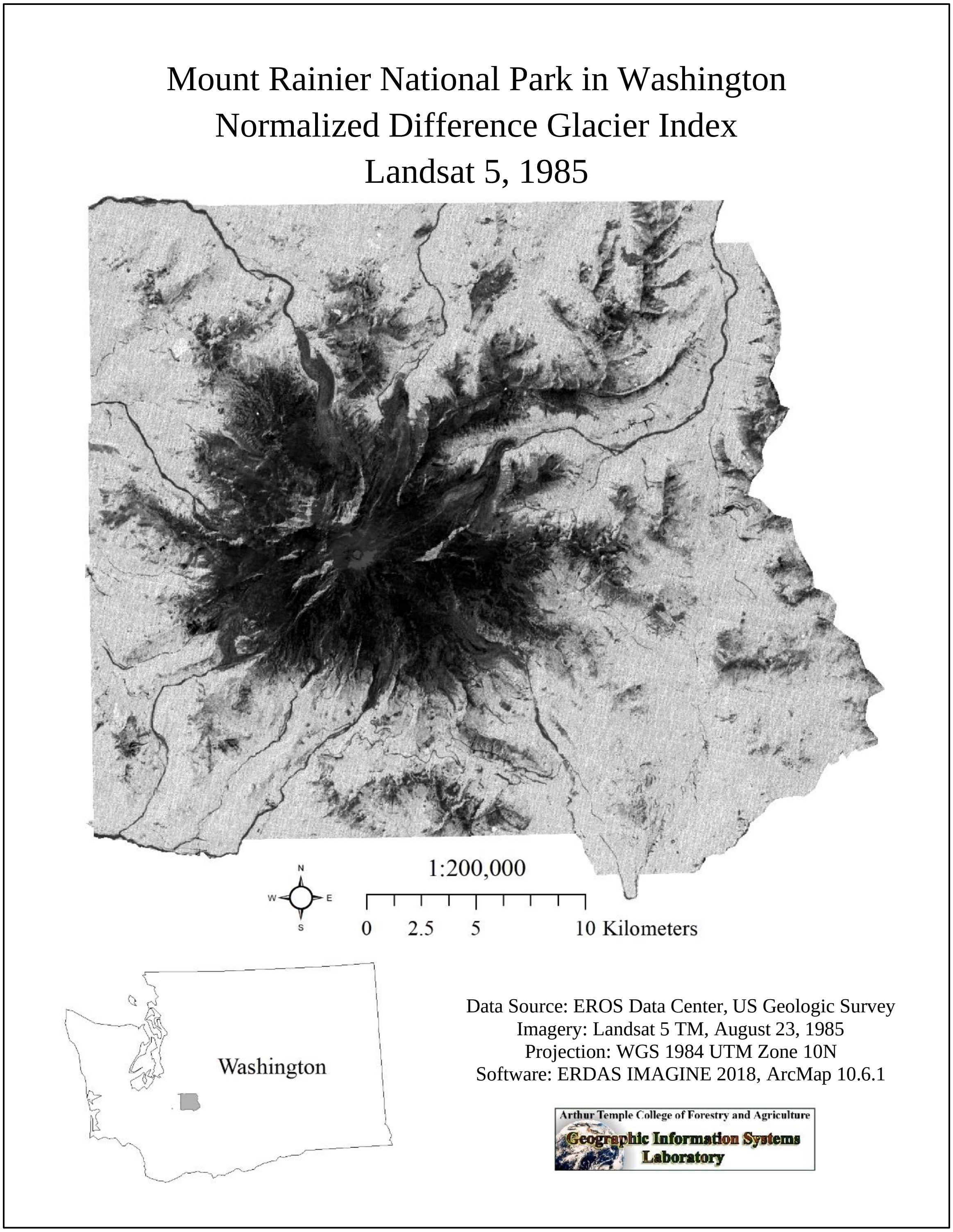

Figure 17. NDGI for Mount Rainier National Park in 1985.

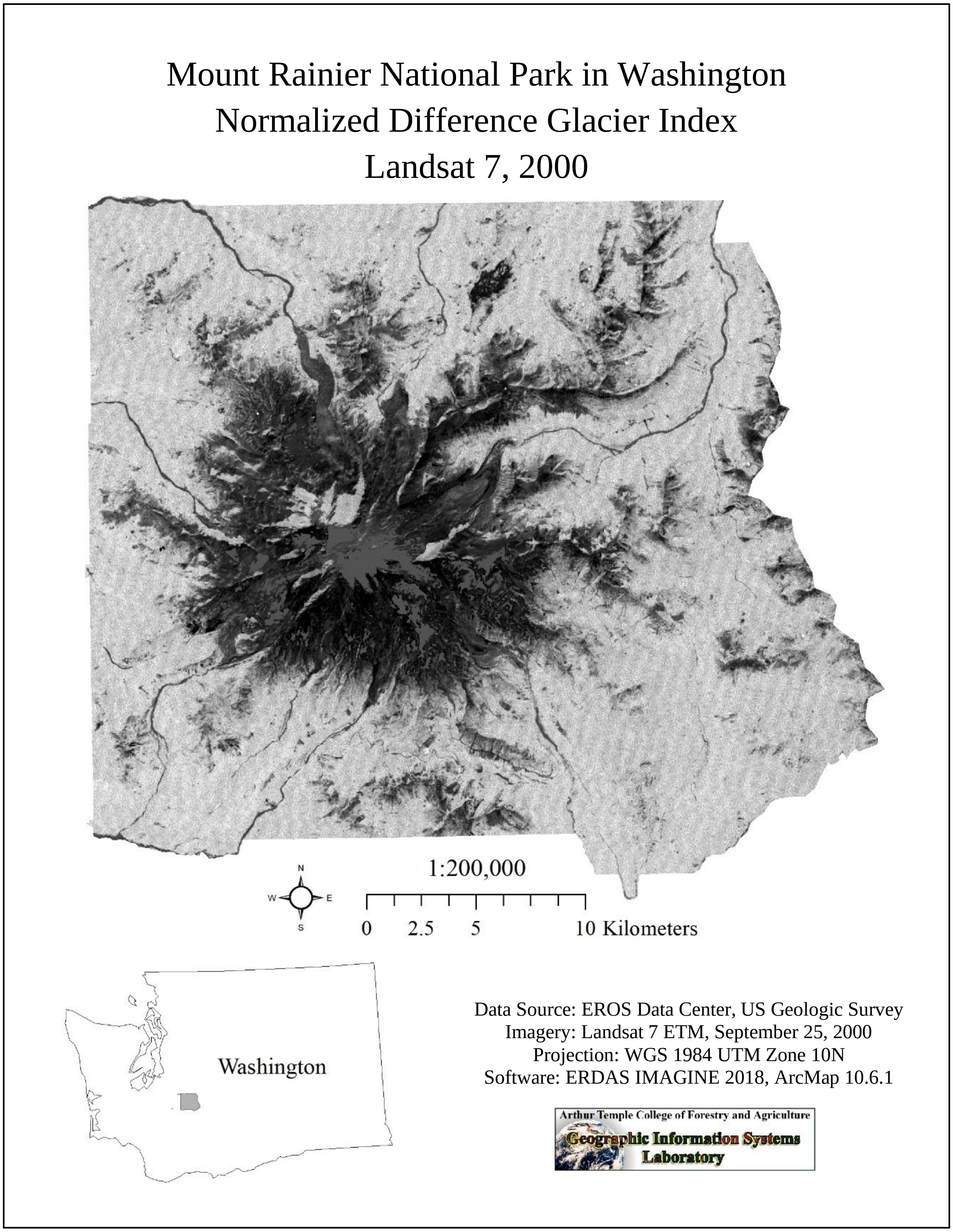

Figure 18. NDGI for Mount Rainier National Park in 2000.

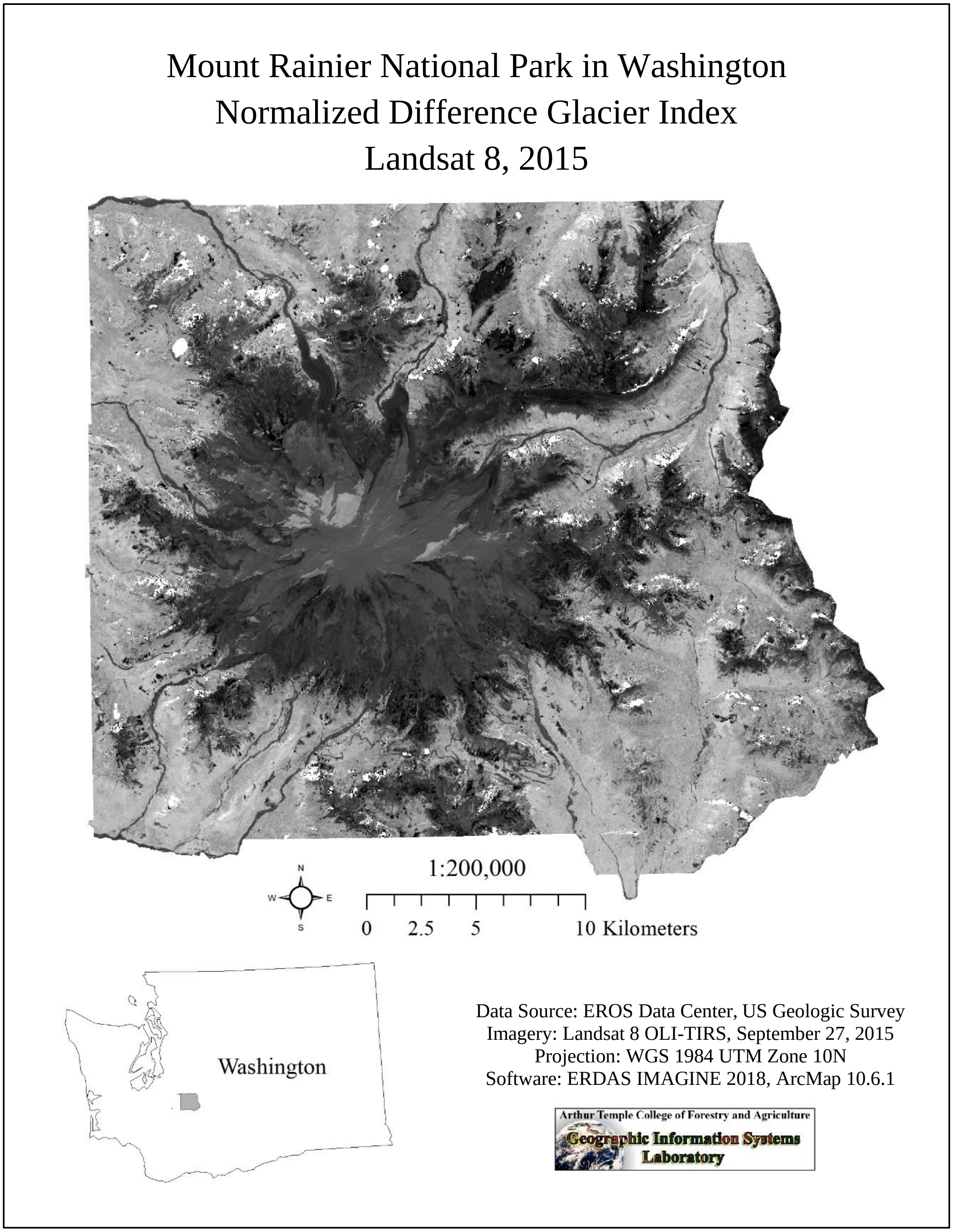

Figure 19. NDGI for Mount Rainier National Park in 2015.

Volume Loss Calculations

In ArcGIS Desktop, a square raster file was generated with an elevation set to zero meters. This file was named "Sea_level". The difference in elevation between the previously created DEMs and "Sea_level" were calculated using the Cut Fill tool (Figure 20). This determined the volume of each DEM. The volume for 2015 was subtracted from the volume in 1985 (or whatever the closest year of topographic maps had been available). The difference was considered the volume of glacier lost between the two years. Actual volume of the glaciers could not be calculated because the underlying bedrock topography was not known for below the glaciers. Figures 21 and 22 display the contour lines digitized from the topographic maps that were used to generate the DEMs for volume loss calculations. Volume loss was not calculated for the 2000 data.

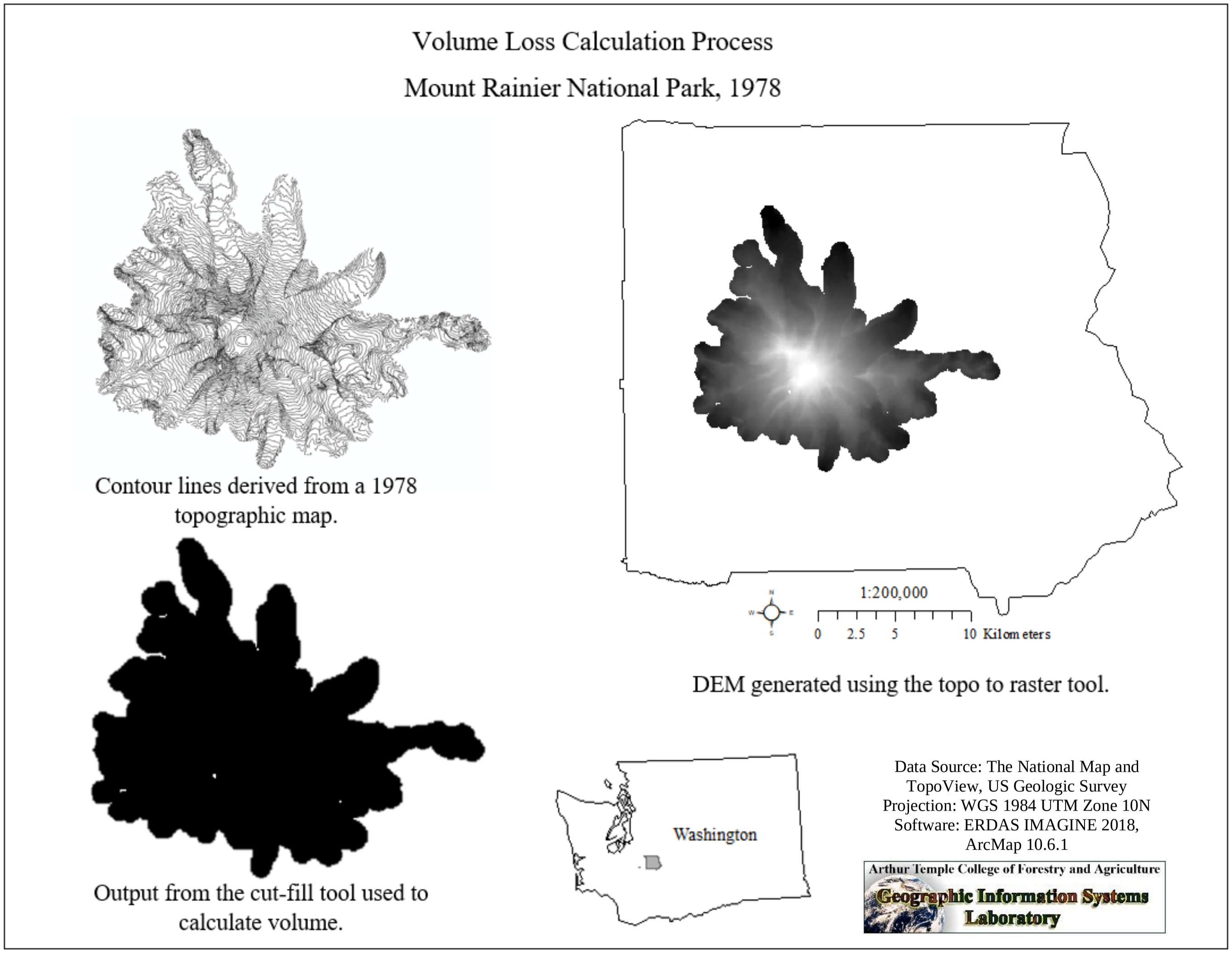

Figure 20. Depiction of the process used to calculate volume loss.

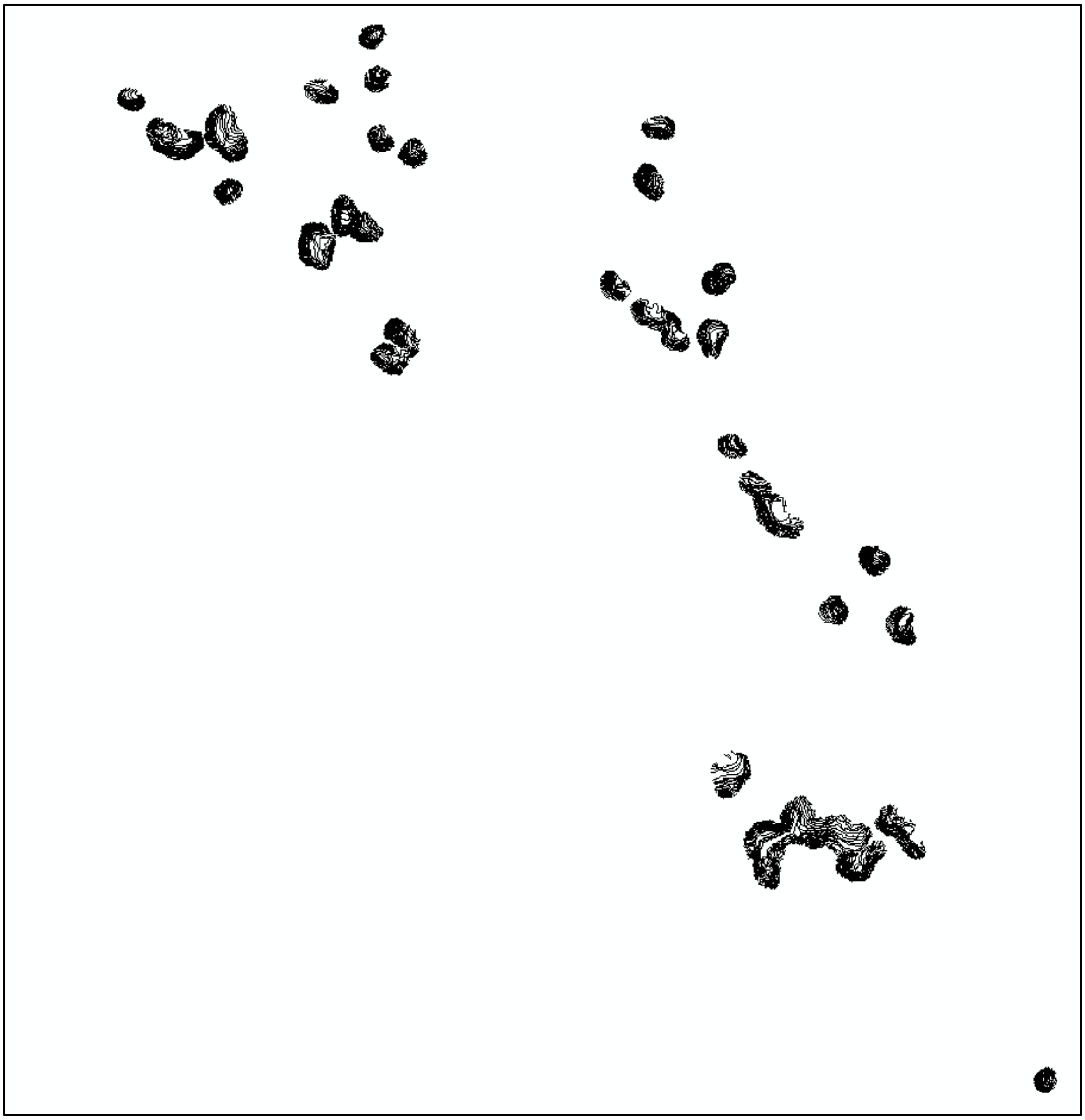

Figure 21. 50 meter contour lines digitized for Glacier National Park from 1981 topographic maps.

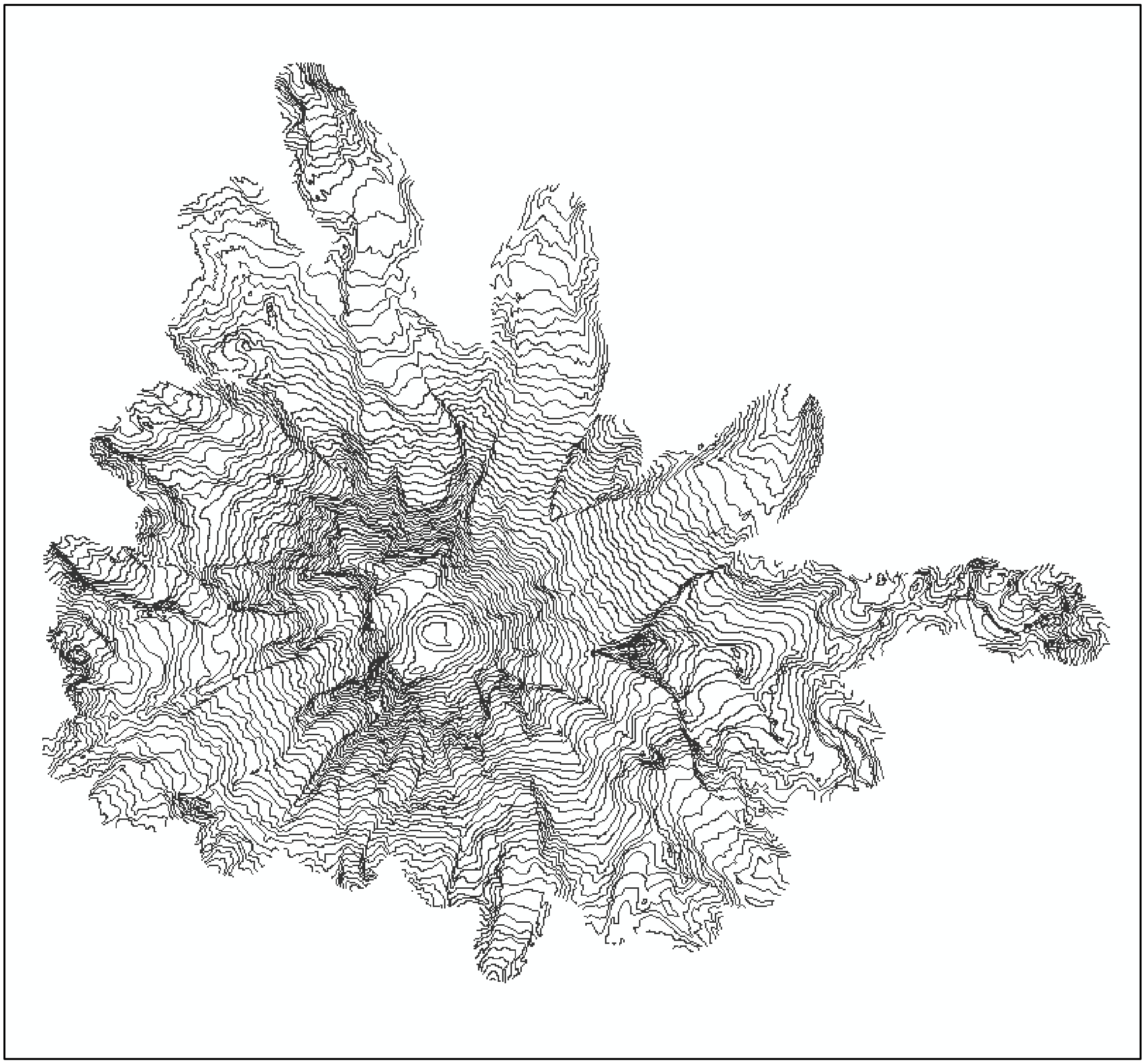

Figure 22. 50 meter contour lines digitized for Mount Rainier National Park from a 1978 topographic map.

Weather Data

Positive Degree Day Sum

Due to the limited availability of weather data, only certain weather parameters were able to be evaluated. The positive degree day sum (PDD) was calculated yearly from 1985 through 2015 using the minimum and maximum temperatures. The PDD is the sum of the degrees above zero degrees Celsius for the measured period. PDD values from multiple years when the years have various numbers of observations could not directly be compared. Some years were missing an entire continuous month of data. The number of observations available for each year period was calculated. The number of observations that were days that the daily temperature were above zero degrees Celsius were also totaled. These daily temperatures were either the daily maximum or minimum according to the PDD being calculated. The PDD was calculated for those days, however this value is unadjusted for missing data. To account for missing data, the number of observations available for the year was divided by the number of days in the year (leap years were accounted for). The result was then subtracted from one to determine the amount of the year missing from the data. The number of days above zero was divided by the total number of observations for the year. This number was then multiplied by the amount of the year missing from the data to get a correction factor that accounted for both the number of observations missing and the number of those missing observations that reasonably would be days above zero. This correction factor was then multiplied by the original PDD to calculate a value to add to the PDD to adjust it to a value that would be more representative of the year.

Cumulative Yearly Snowfall

The total snowfall for each year was added together to get a cumulative sum. The missing days were accounted for. The same method used for PDD was followed excluding the steps accounting for the days above freezing. The East Glacier station was used for Glacier National Park.

RESULTS AND DISCUSSION

Area Calculations

Glacier National Park

The National Park Service published glacier outlines for the years 1966, 1998, and 2015 (NPS, 2017). Their areas were 20.76 km^2, 15.67 km^2, and 13.63 km^2 respectively (Table 6). The areas generated through applying the NDSI were 17.33 km^2 for 1985, 15.80 km^2 for 2000, and 12.56 km^2 for 2015 (Figure 23). From 1985 to 2015, the glaciers decreased in area 27.5 percent. The loss of 3.43 km^2 between 1966 and 1985 is a reasonable amount for the 19 year period based upon a similar difference between 1985 and 2000 as well as 2000 and 2015. The difference in values between 1998 and 2000 can be attributed to fluctuations in annual snowfall. The published extents from 2015 were based on various satellite images, whereas the ones created for this thesis were derived from only one satellite scene.

Table 6. Area of glaciers in Glacier National Park.

Year	Calculated Area (km^2)	Published Area (km^2)
1966	--------	20.76
1985	17.33	--------
1998	--------	15.67
2000	15.80	--------
2015	12.56	13.63

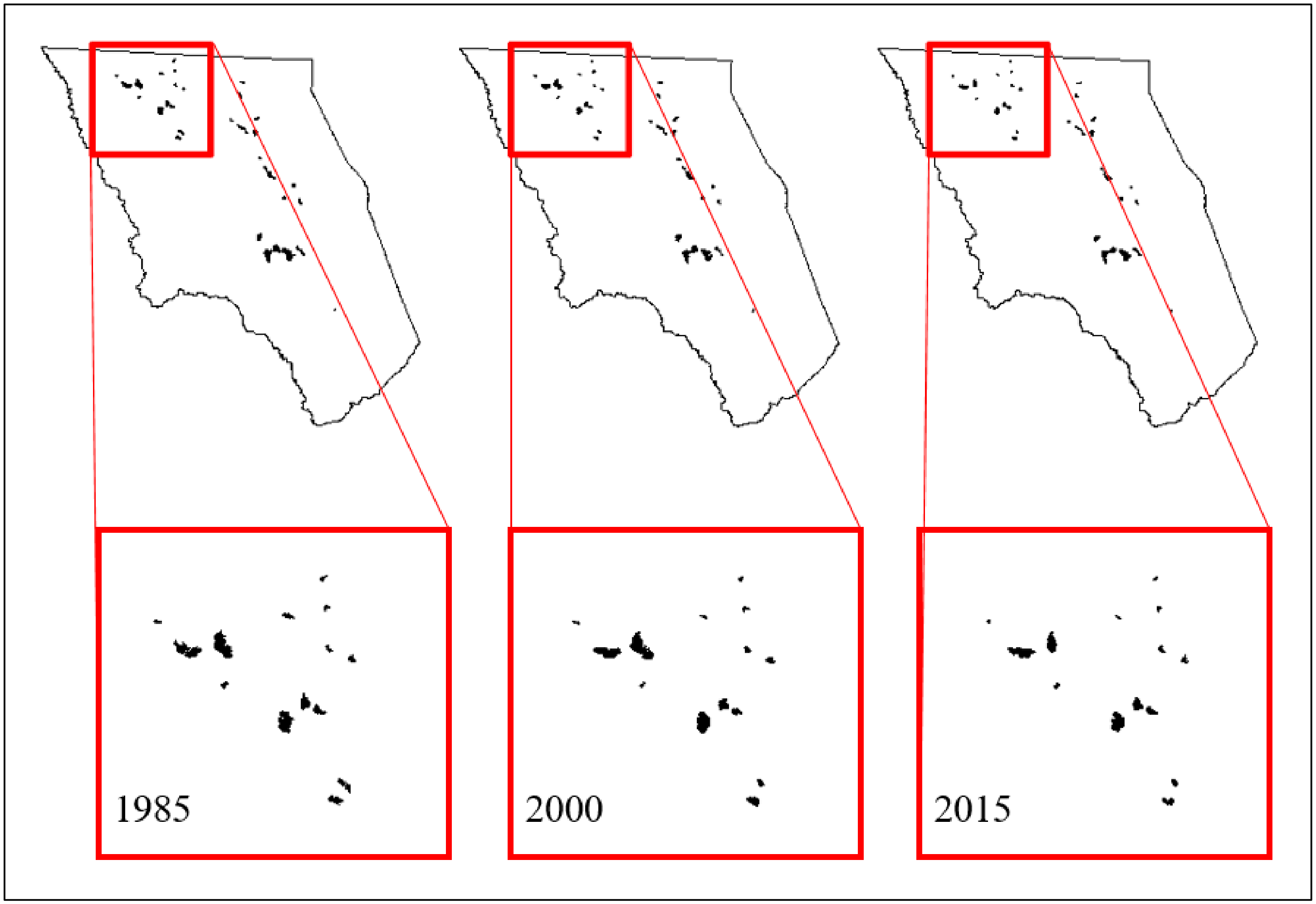

Figure 23. Glacier extents in Glacier National Park.

Many of the differences between the two glacier boundary datasets were located in areas of shadow where visible adjustment could not be properly made without being biased by the accepted outlines.

Mount Rainier National Park

The glacier areas derived for Mount Rainier National Park were 83.39 km^2 (1985), 98.79 km^2 (2000), and 78.67 km^2 (2015) (Table 7; Figure 24). These areas included glacial areas with debris cover and perennial snow fields. The area for the year 2000 was extremely problematic because the perennial snow fields had grown between 1985 and 2000, so whereas they were smaller than 0.05 km^2 in 1985 and therefore deleted, they were larger than 0.05 km^2 by 2000 and not automatically deleted. In order to be consistent in methodology, they were kept and allowed to contribute to the area calculations. Another issue with the perennial snow fields were that various disconnected patches had grown together. The glacier area covered with debris may have had little change between 1985 and 2015 because the debris cover served as insulation for the glacial ice beneath. Instead, changes to the glacier extents/area occurred along the glacier heads closer to Mount Rainier's peak. From 1985 to 2015, the glacier area deceased by 5.7 percent.

Table 7. Area of glaciers in Mount Rainier National Park.

Year	Calculated Area (km^2)	Published Area (km^2)
1985	83.39	--------
2000	98.79	--------
2015	78.67	78.76

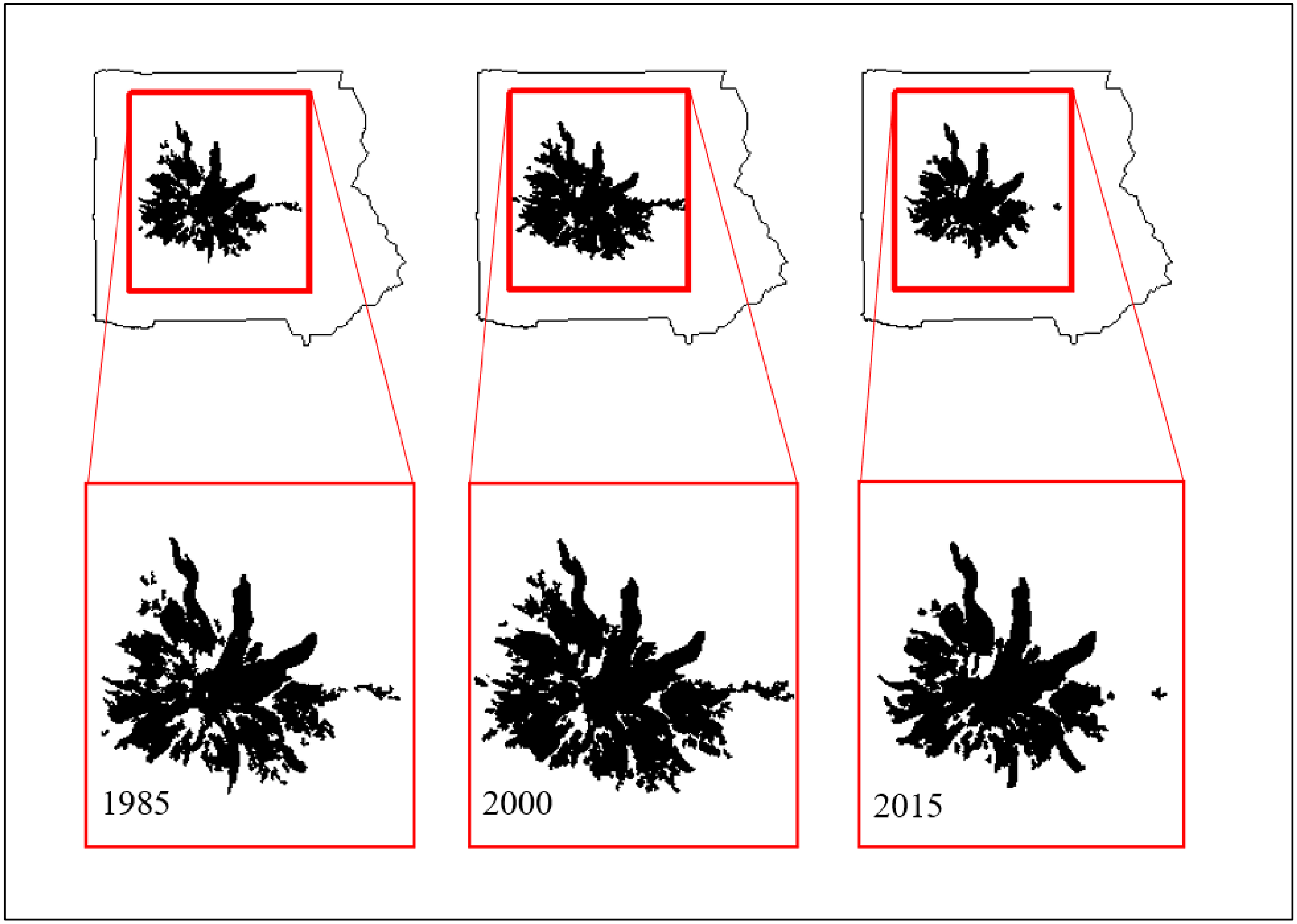

Figure 24. Glacier extents in Mount Rainier National Park.

Volume Loss Calculations

With volume calculations, the exact volume of the glaciers cannot be determined without knowing the topography of the bedrock beneath the glaciers. Without that measurement, it is not possible to calculate the glacier depth remotely. Therefore volume loss calculations were performed by calculating the volume of the glaciers and bedrock at a known point in time and comparing it to another year. The topographic maps used for the initial volumes were limiting due to their contour interval of 50 meters whereas the contour lines downloaded for the more recent years were at intervals of 40 feet. The volume for each year was calculated for the study areas' 1985 glacier extents plus the 500 meter buffer that allowed for the volume of the same size area to be compared. The actual glacier extents could not be used for calculations because they differed between the initial and final year and therefore all of the bedrock below the glaciers would not be consistently counted, which is why the 500 meter buffer was used. By calculating the volume including the buffer, the same amount of bedrock was included in the calculations. For Glacier National Park the 1981 reference volume was 2.3388×10^{11} m^3. This reference volume is not the volume of the glaciers themselves but the volume of the glaciers plus the bedrock below them and including the surrounding 500 meter buffer. All of the bedrock down to sea level was accounted for. The 2011 reference volume was 2.3312×10^{11} m^3, therefore the glaciers in Glacier National Park lost a total of 7.5787×10^{8} m^3 in the thirty year period from 1981 to 2011 (Table 8). This estimate is based on the assumption that any changes in volume within the study area were due to the ablation and accumulation of the glaciers. No studies could be found that had published volume estimations for Glacier National Park. In Mount Rainier National Park the reference volume within the buffer changed from 3.9976×10^{11} m^3 in 1978 to 3.9968×10^{11} m^3. The volume loss for Mount Rainier National Park was 8.5630×10^7 m^3 for the thirty-five year period (Table 9). Jon Waterman (2019) published an article claiming Mount Rainier's glaciers lost 18 percent of their volume since 1970, but the article does not state a specific volume lost. The total volume of the glaciers on Mount Rainier is 4.2×10^9 m^3 in 1994 (Nylen, 2004). Eighteen percent of that volume would be 7.6×10^8 m^3, which largely differs from the estimate of 8.5630×10^7 m^3 calculated based on this study. Therefore the volume loss calculations are limited by the accuracy of the developed DEMs and may not be reflective of actual volume loss.

Table 8. Buffer volumes and volume loss estimate for Glacier National Park.

1981 Volume (m^3)	2011 Volume (m^3)	Volume Loss (m^3)
2.3388E+11	2.3312E+11	7.5787E+08

Table 9. Buffer volumes and volume loss estimate for Mount Rainier National Park

1978 Volume (m^3)	2013 Volume (m^3)	Volume Loss (m^3)
3.9976E+11	3.9968E+11	8.5630E+07

Climate Trends

Clear climate trends exist based on the data for positive degree day (PDD) sums and cumulative annual snowfall. Glacier National Park's PDD based on daily temperature minimums is linearly increasing with an R^2 value of 0.7282 (Table 10; Figure 25). The park's PDD based on daily temperature maximums lacks a strong linear trend, with an R^2 value of 0.0034 (Table 11; Figure 26). For Mount Rainier the PDD based on temperature minimums has a weak positive trend with an R^2 value of 0.0487 (Table 12; Figure 27). However PDD values from 2011 to 2015 were increasing. Using temperature maximums for Mount Rainier, a negative linear trend existed with an R^2 value of 0.0734 (Table 13; Figure 28). PDD values were continuously increasing from 2011 to 2015. Starting in 1994, Glacier National Park has a consistently higher PDD based on temperature minimums (Figure 29). Glacier National Park had a higher PDD based on temperature maximums for every year studied (Figure 30). Higher PDD values correlate to quicker ablation, so based on these trends, Glacier National Park is expected to see larger changes in glacier size. Instead of using daily temperature minimums and maximums, it would have been more beneficial to use daily temperature averages, had they been available.

Within Glacier National Park, a weak positive linear trend existed for cumulative annual snowfall with an R^2 value of 0.0363 (Table 15; Figure 31). Similarly, Mount Rainier also had a weak positive linear trend line with an R^2 value of 0.0992 (Table 15;

Figure 32). Despite having weak linear trends individually, Mount Rainier consistently has two to four times the amount of snowfall in Glacier National Park (Figure 33). Glacier National Park also experiences less drastic differences in snowfall from year to year.

Since Glacier National Park has a higher PDD based on temperature maximums and experienced significantly less snowfall than Mount Rainier, its glacial ablation rates should be higher. This supports the higher percentage of glacier area loss in Glacier National Park.

Table 10. Positive degree day sum for Glacier National Park using the daily temperature minimums.

Year	Total Observations (O)	Days above Zero (DAZ)	PDD	Observation / Days in Year	Year Missing (YM)	DAZ/O	(DAZ/O)* YM	Correction Factor * PDD	Adjusted PDD
1985	N/A	N/A	N/A	N/A	N/A	N/A	N/A	N/A	N/A
1986	339	158	746.2	0.9288	0.0712	0.4661	0.0332	24.7738	770.9738
1987	363	186	901.1	0.9945	0.0055	0.5124	0.0028	2.5300	903.6300
1988	366	172	873.2	1.0000	0.0000	0.4699	0.0000	0.0000	873.2000
1989	365	153	696.6	1.0000	0.0000	0.4192	0.0000	0.0000	696.6000
1990	365	158	758.5	1.0000	0.0000	0.4329	0.0000	0.0000	758.5000
1991	365	147	782.9	1.0000	0.0000	0.4027	0.0000	0.0000	782.9000
1992	366	162	791.4	1.0000	0.0000	0.4426	0.0000	0.0000	791.4000
1993	351	161	610.8	0.9616	0.0384	0.4587	0.0176	10.7462	621.5462
1994	349	164	731.6	0.9562	0.0438	0.4699	0.0206	15.0702	746.6702
1995	365	162	675.6	1.0000	0.0000	0.4438	0.0000	0.0000	675.6000
1996	366	163	782.5	1.0000	0.0000	0.4454	0.0000	0.0000	782.5000
1997	365	178	928.9	1.0000	0.0000	0.4877	0.0000	0.0000	928.9000
1998	365	193	1071.6	1.0000	0.0000	0.5288	0.0000	0.0000	1071.6000
1999	365	193	903.9	1.0000	0.0000	0.5288	0.0000	0.0000	903.9000
2000	366	177	923.4	1.0000	0.0000	0.4836	0.0000	0.0000	923.4000
2001	365	199	1033.2	1.0000	0.0000	0.5452	0.0000	0.0000	1033.2000
2002	365	182	950.7	1.0000	0.0000	0.4986	0.0000	0.0000	950.7000
2003	364	208	1180.9	0.9973	0.0027	0.5714	0.0016	1.8488	1182.7488
2004	366	215	1053.6	1.0000	0.0000	0.5874	0.0000	0.0000	1053.6000
2005	365	222	1129.1	1.0000	0.0000	0.6082	0.0000	0.0000	1129.1000

Table 10. Positive degree day sum for Glacier National Park using the daily temperature minimums (continued).

Year	Total Observations (O)	Days above Zero (DAZ)	PDD	Observation / Days in Year	Year Missing (YM)	DAZ/O	(DAZ/O)* YM	Correction Factor * PDD	Adjusted PDD
2006	365	211	1202.9	1.0000	0.0000	0.5781	0.0000	0.0000	1202.9000
2007	365	218	1208.1	1.0000	0.0000	0.5973	0.0000	0.0000	1208.1000
2008	366	208	1039.3	1.0000	0.0000	0.5683	0.0000	0.0000	1039.3000
2009	365	193	1037.2	1.0000	0.0000	0.5288	0.0000	0.0000	1037.2000
2010	365	217	1094	1.0000	0.0000	0.5945	0.0000	0.0000	1094.0000
2011	365	230	1070.7	1.0000	0.0000	0.6301	0.0000	0.0000	1070.7000
2012	366	213	1162.8	1.0000	0.0000	0.5820	0.0000	0.0000	1162.8000
2013	365	214	1203.9	1.0000	0.0000	0.5863	0.0000	0.0000	1203.9000
2014	365	231	1244.8	1.0000	0.0000	0.6329	0.0000	0.0000	1244.8000
2015	365	228	1333.2	1.0000	0.0000	0.6247	0.0000	0.0000	1333.2000

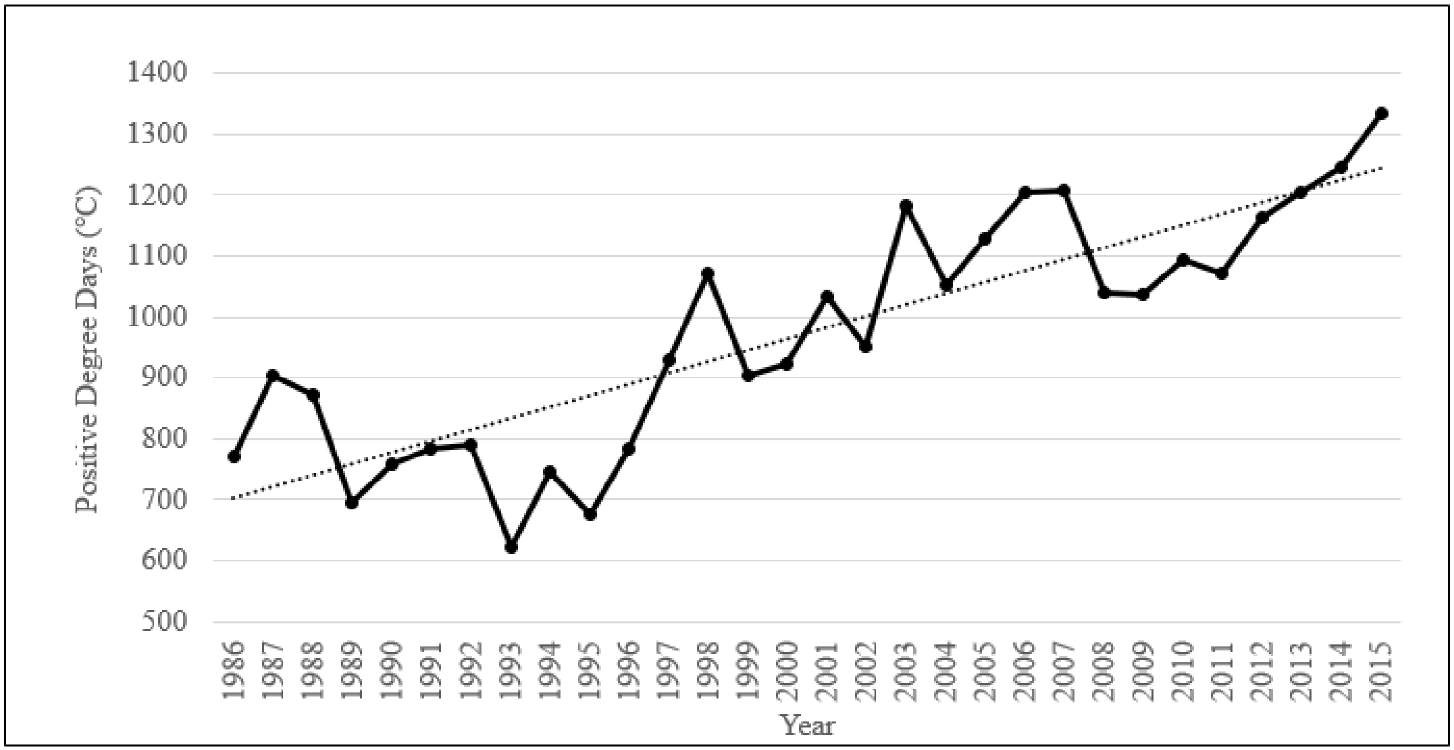

Figure 25. Positive degree day sum for Glacier National Park using the daily temperature minimums.

Table 11. Positive degree day sum for Glacier National Park using the daily temperature maximums.

Year	Total Observations (O)	Days above Zero (DAZ)	PDD	Observation / Days in Year	Year Missing (YM)	DAZ/O	(DAZ/O)* YM	Correction Factor * PDD	Adjusted PDD
1985	N/A	N/A	N/A	N/A	N/A	N/A	N/A	N/A	N/A
1986	339	290	4034.2	0.9288	0.0712	0.8555	0.0609	245.8308	4280.0308
1987	363	304	4316.9	0.9945	0.0055	0.8375	0.0046	19.8096	4336.7096
1988	366	290	4183.8	1.0000	0.0000	0.7923	0.0000	0.0000	4183.8000
1989	365	279	3648.7	1.0000	0.0000	0.7644	0.0000	0.0000	3648.7000
1990	365	288	3986.5	1.0000	0.0000	0.7890	0.0000	0.0000	3986.5000
1991	365	303	3942.1	1.0000	0.0000	0.8301	0.0000	0.0000	3942.1000
1992	366	310	4105.8	1.0000	0.0000	0.8470	0.0000	0.0000	4105.8000
1993	351	285	3532.4	0.9616	0.0384	0.8120	0.0311	110.0127	3642.4127
1994	350	281	4170	0.9589	0.0411	0.8029	0.0330	137.5855	4307.5855
1995	365	317	3753.5	1.0000	0.0000	0.8685	0.0000	0.0000	3753.5000
1996	366	272	3547.2	1.0000	0.0000	0.7432	0.0000	0.0000	3547.2000
1997	365	307	3622.4	1.0000	0.0000	0.8411	0.0000	0.0000	3622.4000
1998	365	320	4180.1	1.0000	0.0000	0.8767	0.0000	0.0000	4180.1000
1999	365	335	3705.8	1.0000	0.0000	0.9178	0.0000	0.0000	3705.8000
2000	366	311	3707.1	1.0000	0.0000	0.8497	0.0000	0.0000	3707.1000
2001	365	318	3918	1.0000	0.0000	0.8712	0.0000	0.0000	3918.0000
2002	365	308	3536.1	1.0000	0.0000	0.8438	0.0000	0.0000	3536.1000
2003	365	315	4139.7	1.0000	0.0000	0.8630	0.0000	0.0000	4139.7000
2004	366	331	3875.5	1.0000	0.0000	0.9044	0.0000	0.0000	3875.5000
2005	365	318	3955	1.0000	0.0000	0.8712	0.0000	0.0000	3955.0000

Table 11. Positive degree day sum for Glacier National Park using the daily temperature maximums (continued).

Year	Total Observations (O)	Days above Zero (DAZ)	PDD	Observation / Days in Year	Year Missing (YM)	DAZ/O	(DAZ/O)* YM	Correction Factor * PDD	Adjusted PDD
2006	365	325	4249.4	1.0000	0.0000	0.8904	0.0000	0.0000	4249.4000
2007	365	316	4216.6	1.0000	0.0000	0.8658	0.0000	0.0000	4216.6000
2008	366	316	3909.1	1.0000	0.0000	0.8634	0.0000	0.0000	3909.1000
2009	365	306	3905.6	1.0000	0.0000	0.8384	0.0000	0.0000	3905.6000
2010	365	329	3898	1.0000	0.0000	0.9014	0.0000	0.0000	3898.0000
2011	365	315	3744.5	1.0000	0.0000	0.8630	0.0000	0.0000	3744.5000
2012	366	315	4057.5	1.0000	0.0000	0.8607	0.0000	0.0000	4057.5000
2013	365	331	4067.2	1.0000	0.0000	0.9068	0.0000	0.0000	4067.2000
2014	365	320	4049.9	1.0000	0.0000	0.8767	0.0000	0.0000	4049.9000
2015	365	327	4447.9	1.0000	0.0000	0.8959	0.0000	0.0000	4447.9000

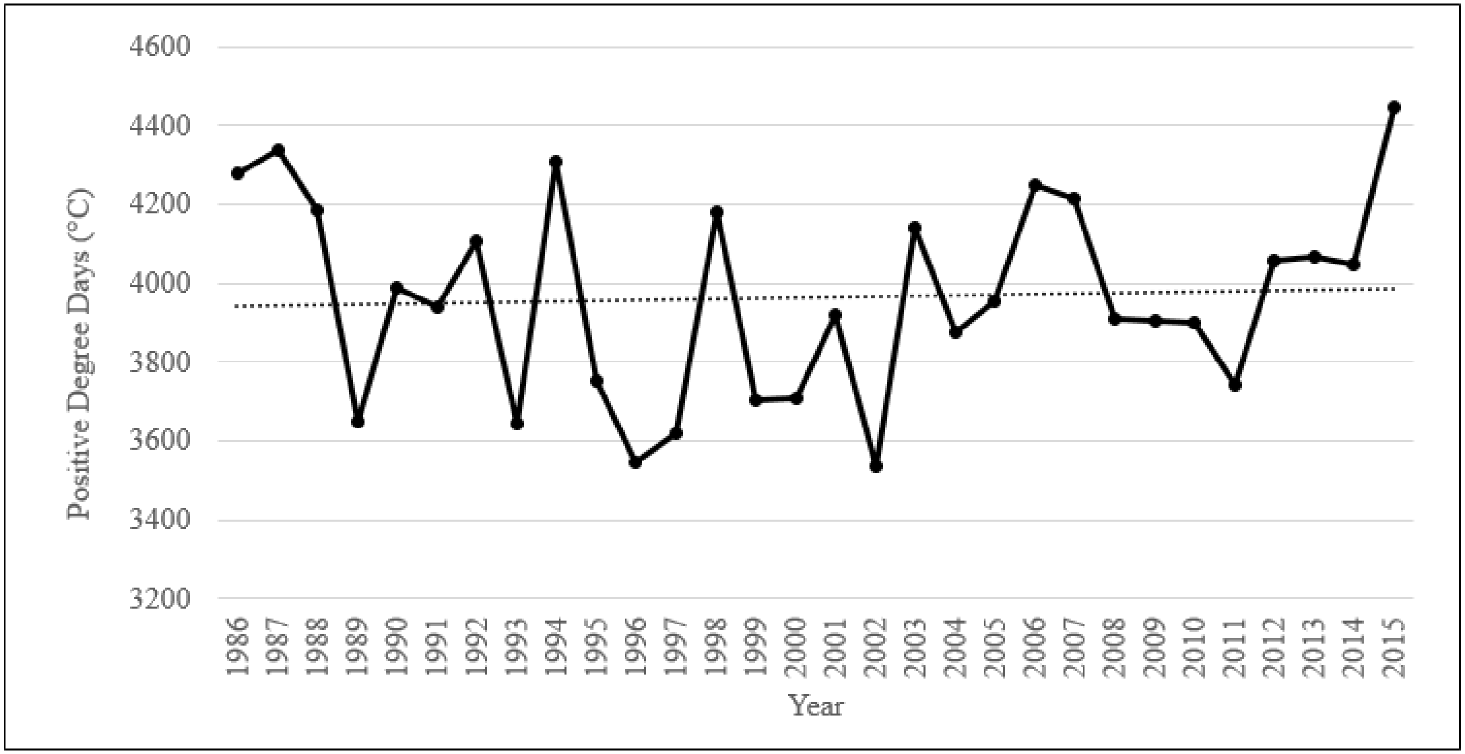

Figure 26. Positive degree day sum for Glacier National Park using the daily temperature maximums.

Table 12. Positive degree day sum for Mount Rainier National Park using the daily temperature minimums.

Year	Total Observations (O)	Days above Zero (DAZ)	PDD	Observation / Days in Year	Year Missing (YM)	DAZ/O	(DAZ/O)* YM	Correction Factor * PDD	Adjusted PDD
1985	364	146	752.7	0.9973	0.0027	0.4011	0.0011	0.8271	753.5271
1986	365	156	958	1.0000	0.0000	0.4274	0.0000	0.0000	958.0000
1987	330	165	967.1	0.9041	0.0959	0.5000	0.0479	46.3678	1013.4678
1988	365	140	850.1	0.9973	0.0027	0.3836	0.0010	0.8909	850.9909
1989	362	155	729.2	0.9918	0.0082	0.4282	0.0035	2.5662	731.7662
1990	355	132	651.6	0.9726	0.0274	0.3718	0.0102	6.6379	658.2379
1991	365	147	798.2	1.0000	0.0000	0.4027	0.0000	0.0000	798.2000
1992	366	157	916.7	1.0000	0.0000	0.4290	0.0000	0.0000	916.7000
1993	365	124	562.6	1.0000	0.0000	0.3397	0.0000	0.0000	562.6000
1994	303	126	672.3	0.8301	0.1699	0.4158	0.0706	47.4887	719.7887
1995	315	122	544.6	0.8630	0.1370	0.3873	0.0531	28.8938	573.4938
1996	273	104	579.7	0.7459	0.2541	0.3810	0.0968	56.1146	635.8146
1997	310	105	588.5	0.8493	0.1507	0.3387	0.0510	30.0361	618.5361
1998	354	147	962.8	0.9699	0.0301	0.4153	0.0125	12.0490	974.8490
1999	330	109	676	0.9041	0.0959	0.3303	0.0317	21.4109	697.4109
2000	329	103	435.2	0.8989	0.1011	0.3131	0.0316	13.7737	448.9737
2001	349	131	778.8	0.9562	0.0438	0.3754	0.0165	12.8144	791.6144
2002	347	151	874.7	0.9507	0.0493	0.4352	0.0215	18.7709	893.4709
2003	248	87	486.8	0.6795	0.3205	0.3508	0.1125	54.7408	541.5408
2004	337	153	958.6	0.9208	0.0792	0.4540	0.0360	34.4839	993.0839
2005	348	168	851.8	0.9534	0.0466	0.4828	0.0225	19.1524	870.9524

Table 12. Positive degree day sum for Mount Rainier National Park using the daily temperature minimums (continued).

Year	Total Observations (O)	Days above Zero (DAZ)	PDD	Observation Days in Year	Year Missing (YM)	DAZ/O	(DAZ/O)* YM	Correction Factor * PDD	Adjusted PDD
2006	330	129	811.4	0.9041	0.0959	0.3909	0.0375	30.4149	841.8149
2007	325	145	784.7	0.8904	0.1096	0.4462	0.0489	38.3668	823.0668
2008	256	88	499.7	0.6995	0.3005	0.3438	0.1033	51.6254	551.3254
2009	290	113	578.1	0.7945	0.2055	0.3897	0.0801	46.2862	624.3862
2010	330	143	796.3	0.9041	0.0959	0.4333	0.0416	33.0883	829.3883
2011	348	116	597.4	0.9534	0.0466	0.3333	0.0155	9.2747	606.6747
2012	334	136	891	0.9126	0.0874	0.4072	0.0356	31.7204	922.7204
2013	319	150	970.8	0.8740	0.1260	0.4702	0.0593	57.5301	1028.3301
2014	312	160	944.3	0.8548	0.1452	0.5128	0.0745	70.3167	1014.6167
2015	340	194	1279.1	0.9315	0.0685	0.5706	0.0391	49.9890	1329.0890

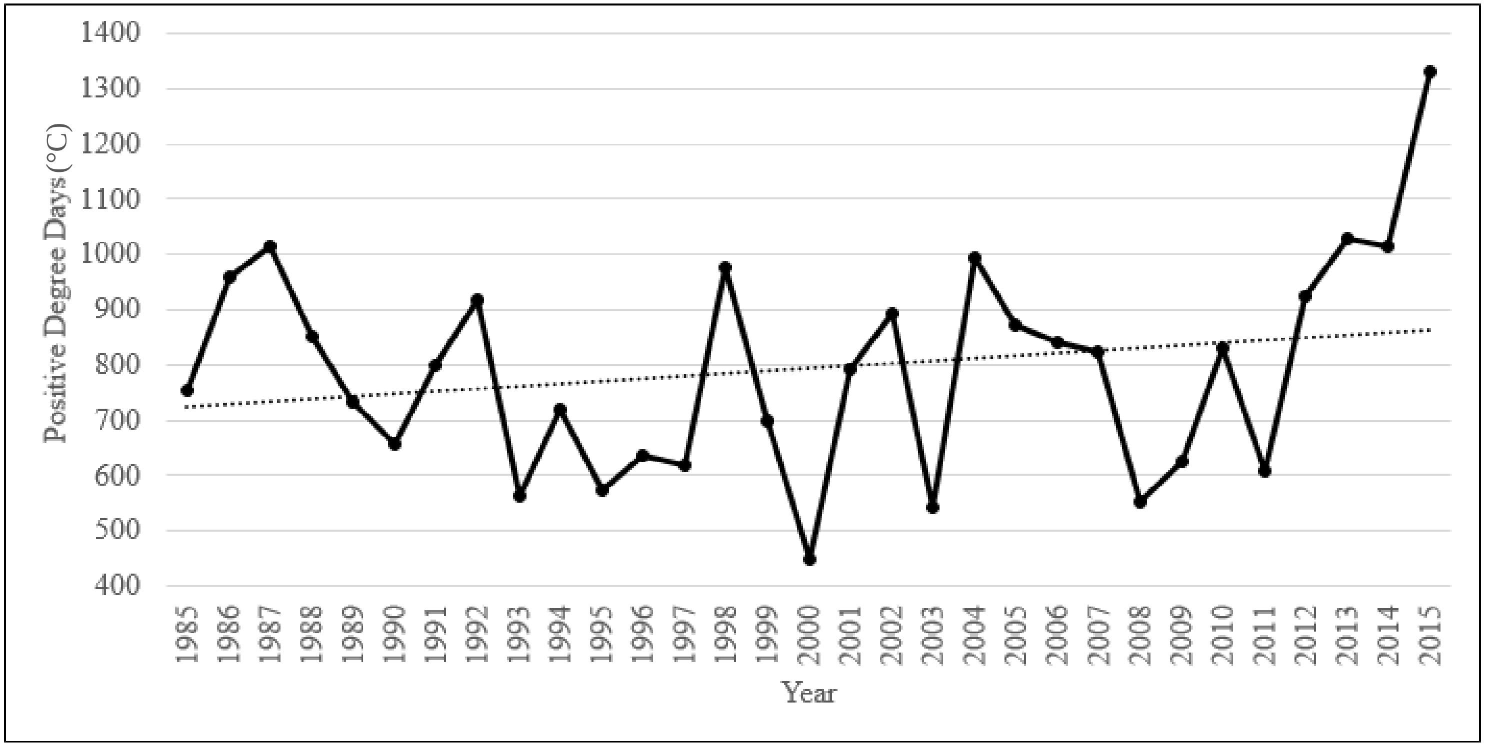

Figure 27. Positive degree day sum for Mount Rainier National Park using the daily temperature minimums.

Table 13. Positive degree day sum for Mount Rainier National Park using the daily temperature maximums.

Year	Total Observations (O)	Days above Zero (DAZ)	PDD	Observation / Days in Year	Year Missing (YM)	DAZ/O	(DAZ/O)* YM	Correction Factor * PDD	Adjusted PDD
1985	363	278	2885.6	0.9945	0.0055	0.7658	0.0042	12.1091	2897.7091
1986	365	308	3169	1.0000	0.0000	0.8438	0.0000	0.0000	3169.0000
1987	329	280	3337	0.9014	0.0986	0.8511	0.0839	280.1096	3617.1096
1988	365	282	3204.4	0.9973	0.0027	0.7726	0.0021	6.7643	3211.1643
1989	362	291	2872.5	0.9918	0.0082	0.8039	0.0066	18.9790	2891.4790
1990	355	276	3045.6	0.9726	0.0274	0.7775	0.0213	64.8725	3110.4725
1991	365	291	2940.7	1.0000	0.0000	0.7973	0.0000	0.0000	2940.7000
1992	364	297	3368.5	0.9945	0.0055	0.8159	0.0045	15.0190	3383.5190
1993	365	292	2717.9	1.0000	0.0000	0.8000	0.0000	0.0000	2717.9000
1994	303	220	2422.3	0.8301	0.1699	0.7261	0.1233	298.7492	2721.0492
1995	315	262	2278	0.8630	0.1370	0.8317	0.1139	259.5503	2537.5503
1996	273	215	2375.4	0.7459	0.2541	0.7875	0.2001	475.3510	2850.7510
1997	310	242	2115.5	0.8493	0.1507	0.7806	0.1176	248.8494	2364.3494
1998	354	267	2783.4	0.9699	0.0301	0.7542	0.0227	63.2679	2846.6679
1999	330	237	2534.4	0.9041	0.0959	0.7182	0.0689	174.5359	2708.9359
2000	329	242	2390.8	0.8989	0.1011	0.7356	0.0744	177.7802	2568.5802
2001	349	252	2777.7	0.9562	0.0438	0.7221	0.0317	87.9200	2865.6200
2002	347	261	2617.7	0.9507	0.0493	0.7522	0.0371	97.0981	2714.7981
2003	248	186	1702.8	0.6795	0.3205	0.7500	0.2404	409.3718	2112.1718
2004	337	271	2834.5	0.9208	0.0792	0.8042	0.0637	180.6062	3015.1062
2005	347	275	2728.7	0.9507	0.0493	0.7925	0.0391	106.6445	2835.3445

Table 13. Positive degree day sum for Mount Rainier National Park using the daily temperature maximums (continued).

Year	Total Observations (O)	Days above Zero (DAZ)	PDD	Observation / Days in Year	Year Missing (YM)	DAZ/O	(DAZ/O)* YM	Correction Factor * PDD	Adjusted PDD
2006	329	248	2643	0.9014	0.0986	0.7538	0.0743	196.5000	2839.5000
2007	325	264	2470.7	0.8904	0.1096	0.8123	0.0890	219.9418	2690.6418
2008	256	175	1734	0.6995	0.3005	0.6836	0.2055	356.2532	2090.2532
2009	290	229	2218.6	0.7945	0.2055	0.7897	0.1623	359.9854	2578.5854
2010	330	271	2700.9	0.9041	0.0959	0.8212	0.0787	212.6861	2913.5861
2011	348	248	2284.7	0.9534	0.0466	0.7126	0.0332	75.8329	2360.5329
2012	334	244	2607.6	0.9126	0.0874	0.7305	0.0639	166.5533	2774.1533
2013	319	255	2673.9	0.8740	0.1260	0.7994	0.1007	269.3765	2943.2765
2014	312	252	2687.6	0.8548	0.1452	0.8077	0.1173	315.2054	3002.8054
2015	338	302	3342.7	0.9260	0.0740	0.8935	0.0661	220.9320	3563.6320

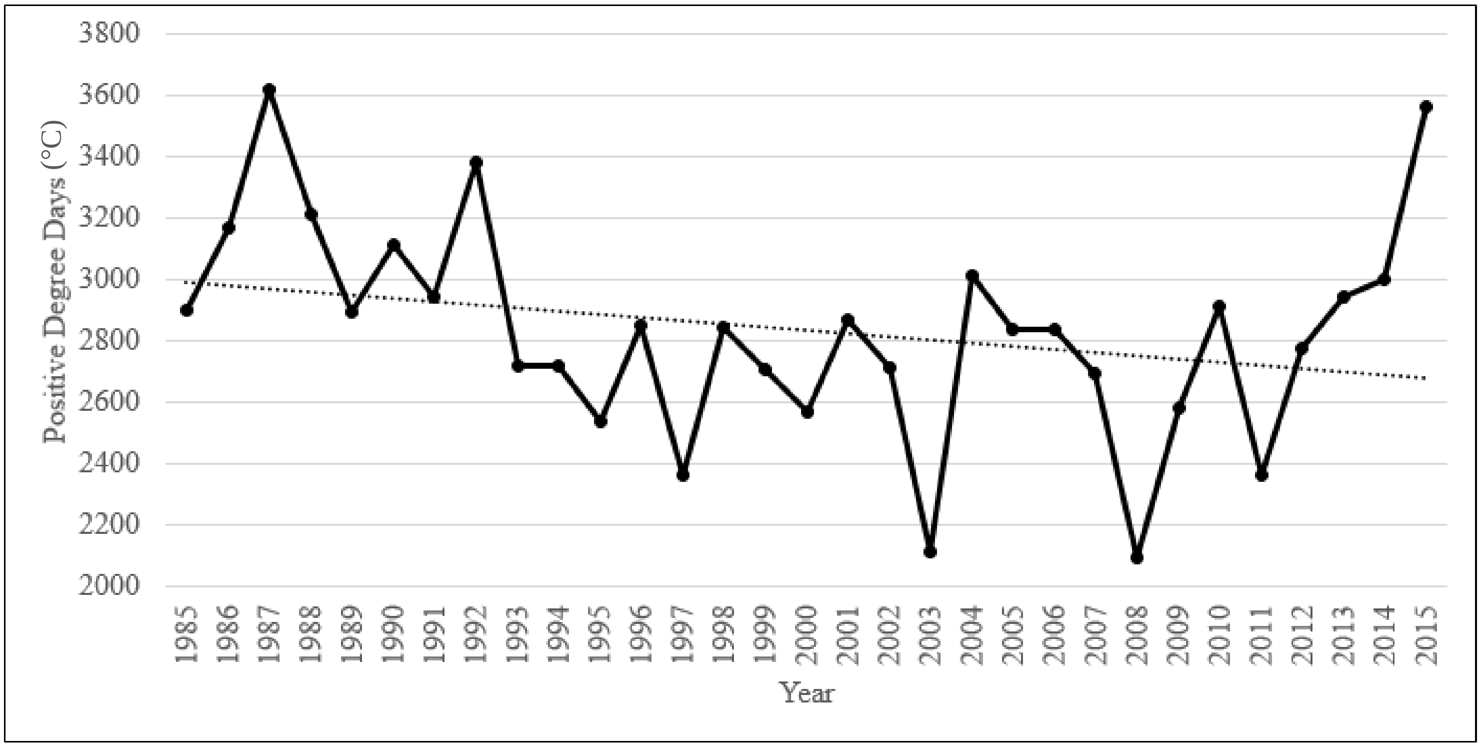

Figure 28. Positive degree day sum for Mount Rainier National Park using the daily temperature maximums.

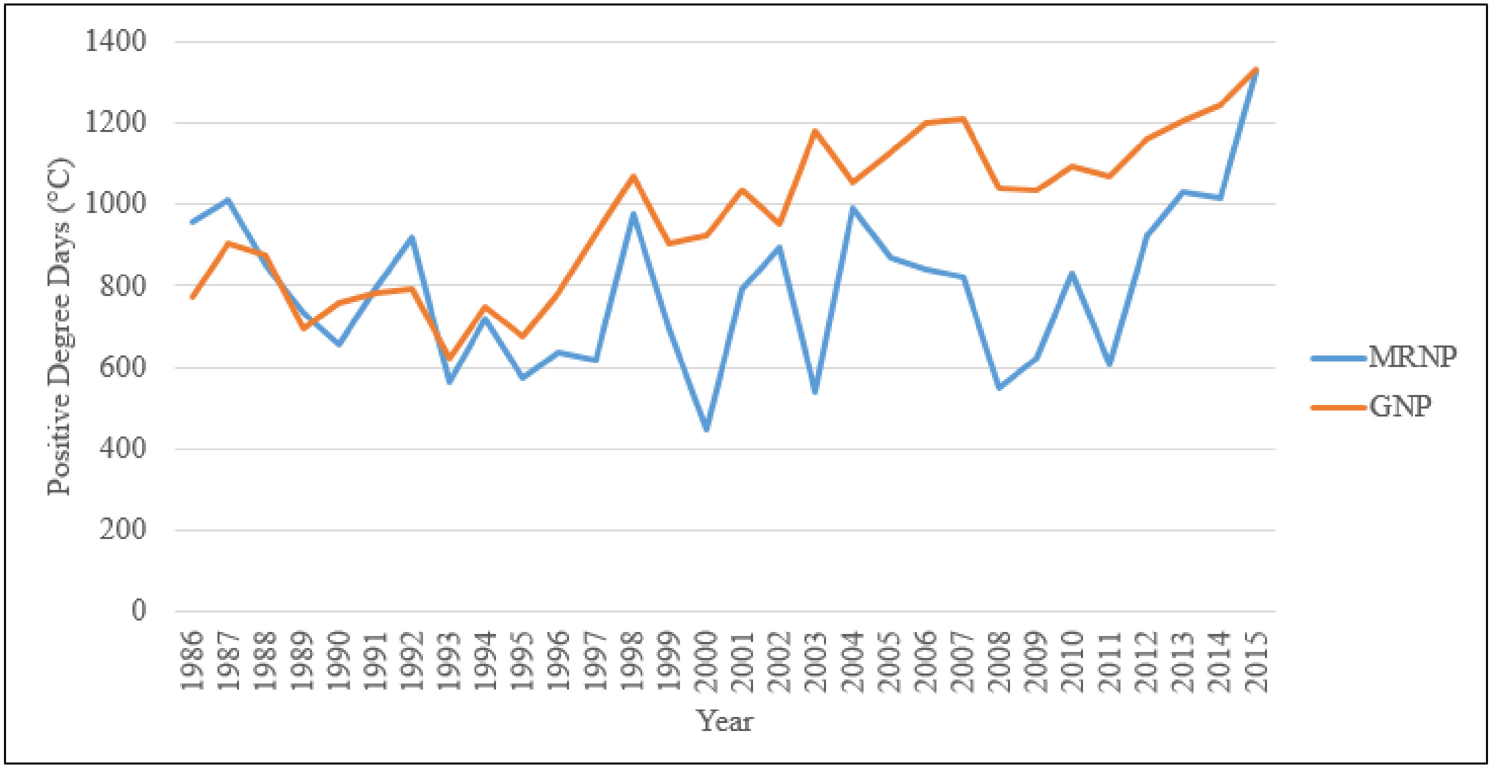

Figure 29. Comparison of the positive degree day sums for Glacier National Park and Mount Rainier National Park based on the daily temperature minimums.

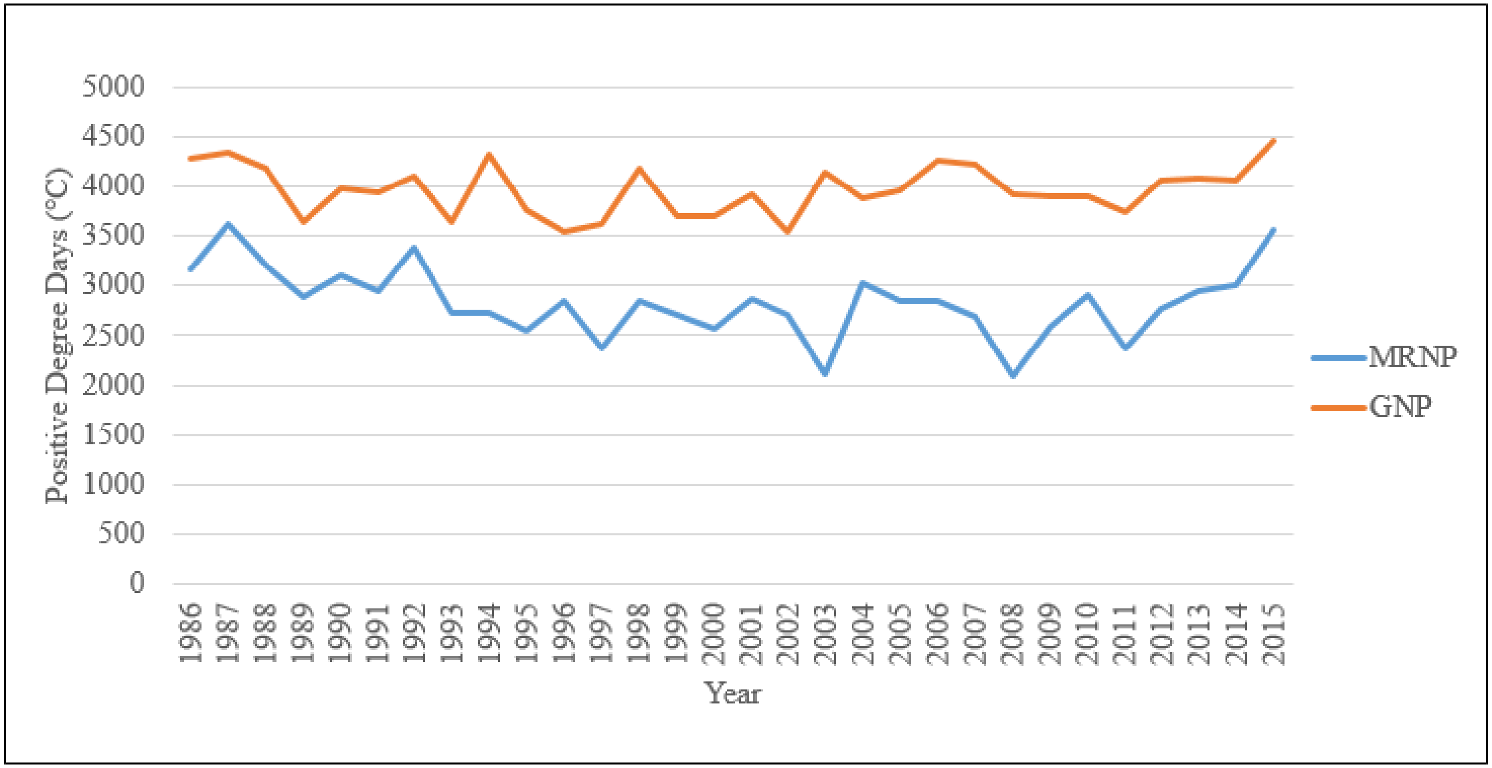

Figure 30. Comparison of the positive degree day sums for Glacier National Park and Mount Rainier National Park based on the daily temperature maximums.

Table 14. Cumulative sum of snowfall in millimeters for Glacier National Park per year.

Year	Total Observations	Snowfall (mm)	Observation Days in Year	Year Missing (YM)	YM * Snowfall	Adjusted Snowfall (mm)
1985	342	4056	0.9370	0.0630	255.5836	4311.5836
1986	351	4060	0.9616	0.0384	155.7260	4215.7260
1987	365	2477	1.0000	0.0000	0.0000	2477.0000
1988	351	3296	0.9590	0.0410	135.0820	3431.0820
1989	351	5130	0.9616	0.0384	196.7671	5326.7671
1990	329	5507	0.9014	0.0986	543.1562	6050.1562
1991	330	3454	0.9041	0.0959	331.2055	3785.2055
1992	322	2689	0.8798	0.1202	323.2678	3012.2678
1993	295	2157	0.8082	0.1918	413.6712	2570.6712
1994	305	2357	0.8356	0.1644	387.4521	2744.4521
1995	356	2348	0.9753	0.0247	57.8959	2405.8959
1996	344	6092	0.9399	0.0601	366.1858	6458.1858
1997	360	2676	0.9863	0.0137	36.6575	2712.6575
1998	237	4399	0.6493	0.3507	1542.6630	5941.6630
1999	349	4012	0.9562	0.0438	175.8685	4187.8685
2000	363	3188	0.9918	0.0082	26.1311	3214.1311
2001	333	3327	0.9123	0.0877	291.6822	3618.6822
2002	364	6869	0.9973	0.0027	18.8192	6887.8192
2003	365	4173	1.0000	0.0000	0.0000	4173.0000
2004	357	3662	0.9754	0.0246	90.0492	3752.0492
2005	329	3326	0.9014	0.0986	328.0438	3654.0438
2006	310	3153	0.8493	0.1507	475.1096	3628.1096
2007	355	3013	0.9726	0.0274	82.5479	3095.5479
2008	348	4329	0.9508	0.0492	212.9016	4541.9016
2009	362	5392	0.9918	0.0082	44.3178	5436.3178
2010	365	2823	1.0000	0.0000	0.0000	2823.0000
2011	355	4957	0.9726	0.0274	135.8082	5092.8082
2012	338	4366	0.9235	0.0765	334.0109	4700.0109
2013	357	4799	0.9781	0.0219	105.1836	4904.1836
2014	309	5033	0.8466	0.1534	772.1863	5805.1863
2015	271	3074	0.7425	0.2575	791.6603	3865.6603

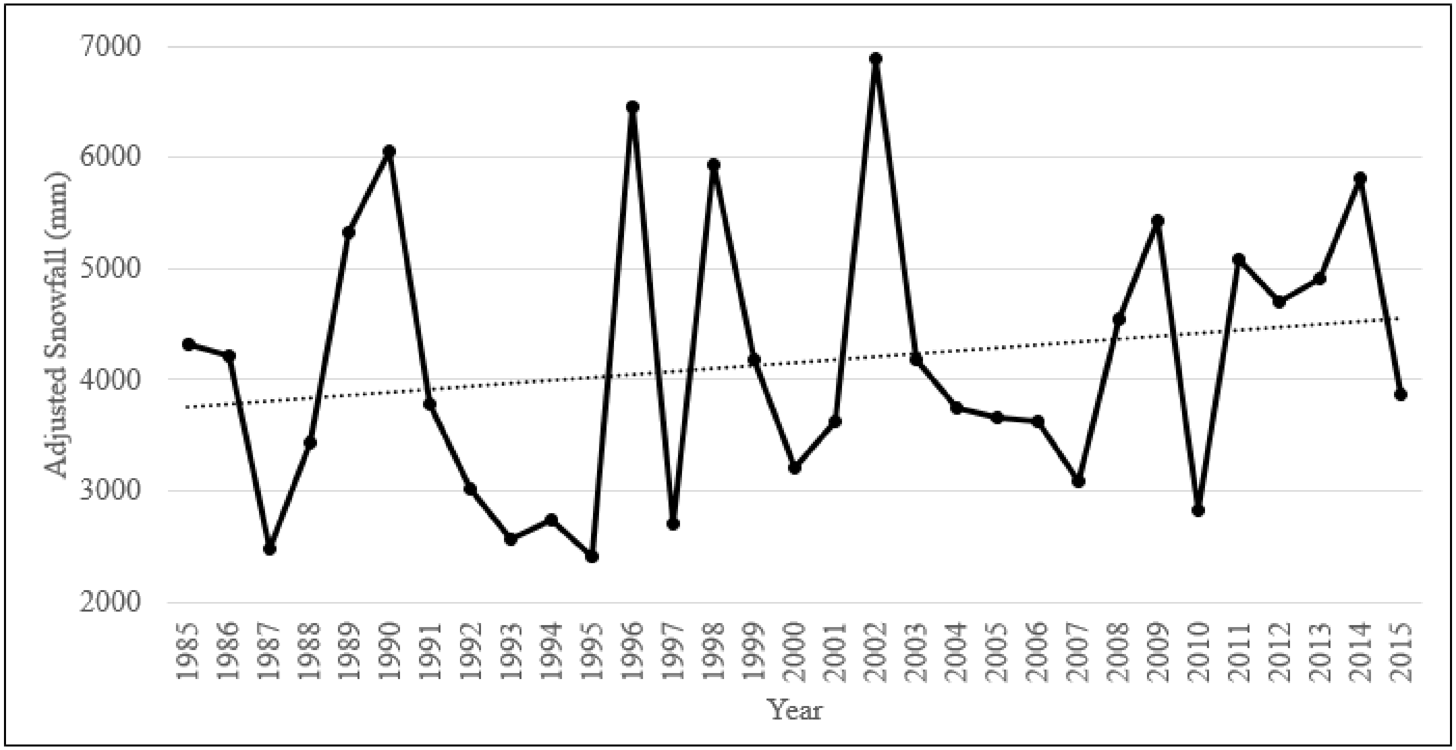

Figure 31. Cumulative sum of snowfall in millimeters for Glacier National Park per year.

Table 15. Cumulative sum of snowfall in millimeters for Mount Rainier National Park per year.

Year	Total Observations	Snowfall (mm)	Observation Days in Year	Year Missing (YM)	YM * Snowfall	Adjusted Snowfall (mm)
1985	364	13402	0.9973	0.0027	36.7178	13438.7178
1986	365	15049	1.0000	0.0000	0.0000	15049.0000
1987	332	10531	0.9096	0.0904	952.1178	11483.1178
1988	364	18620	0.9945	0.0055	101.7486	18721.7486
1989	364	14757	0.9973	0.0027	40.4301	14797.4301
1990	360	20080	0.9863	0.0137	275.0685	20355.0685
1991	364	18429	0.9973	0.0027	50.4904	18479.4904
1992	355	13353	0.9699	0.0301	401.3197	13754.3197
1993	363	10187	0.9945	0.0055	55.8192	10242.8192
1994	303	19736	0.8301	0.1699	3352.4164	23088.4164
1995	360	12602	0.9863	0.0137	172.6301	12774.6301
1996	303	15164	0.8279	0.1721	2610.1967	17774.1967
1997	319	16850	0.8740	0.1260	2123.5616	18973.5616
1998	361	20365	0.9890	0.0110	223.1781	20588.1781
1999	352	21556	0.9644	0.0356	767.7479	22323.7479
2000	356	14419	0.9727	0.0273	393.9617	14812.9617
2001	363	18008	0.9945	0.0055	98.6740	18106.6740
2002	361	16417	0.9890	0.0110	179.9123	16596.9123
2003	332	15885	0.9096	0.0904	1436.1781	17321.1781
2004	349	11222	0.9536	0.0464	521.2404	11743.2404
2005	362	13072	0.9918	0.0082	107.4411	13179.4411
2006	358	19959	0.9808	0.0192	382.7753	20341.7753
2007	334	14140	0.9151	0.0849	1200.9315	15340.9315
2008	337	21331	0.9208	0.0792	1690.1612	23021.1612
2009	288	15514	0.7890	0.2110	3272.8164	18786.8164
2010	311	13893	0.8521	0.1479	2055.4027	15948.4027
2011	307	20062	0.8411	0.1589	3187.9342	23249.9342
2012	302	20970	0.8251	0.1749	3666.8852	24636.8852
2013	273	13173	0.7479	0.2521	3320.3178	16493.3178
2014	280	15010	0.7671	0.2329	3495.4795	18505.4795
2015	243	11766	0.6658	0.3342	3932.7452	15698.7452

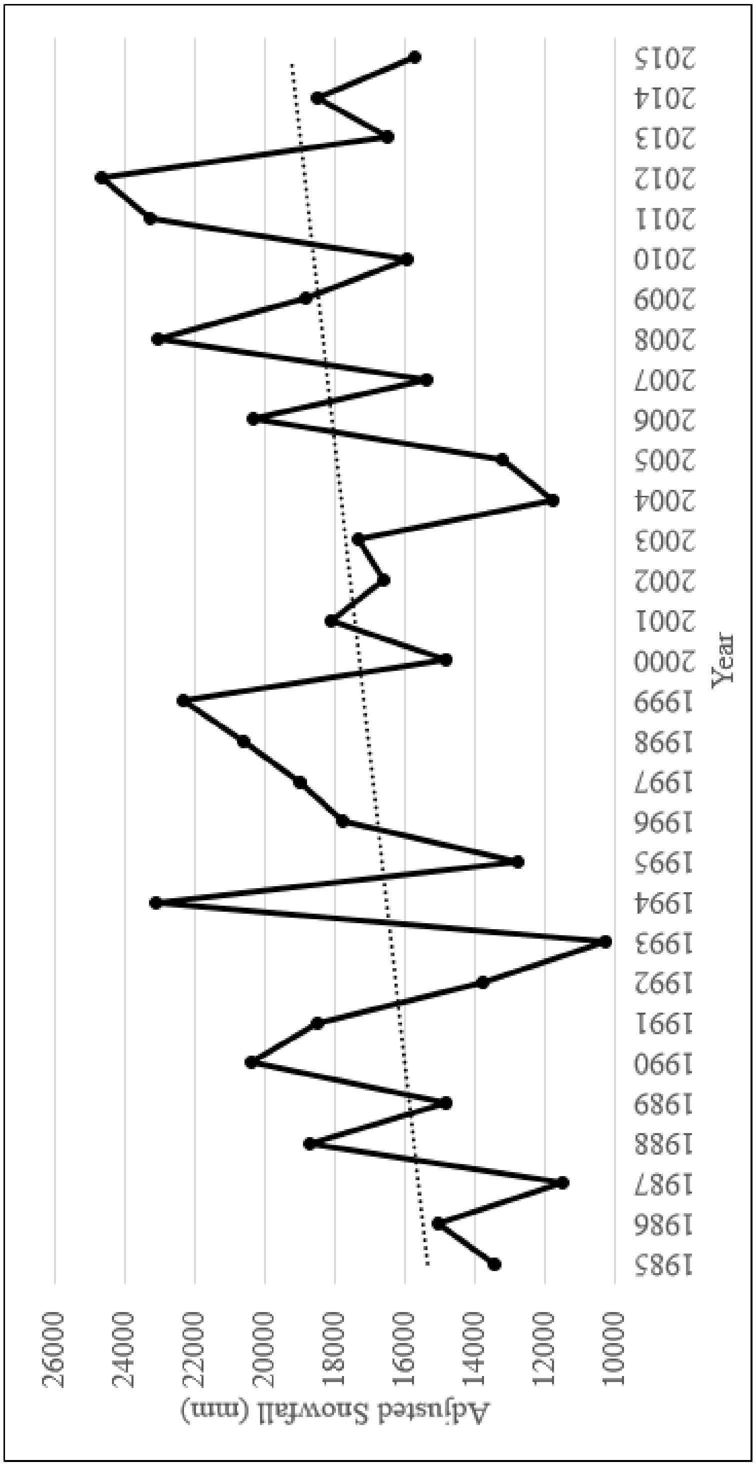

Figure 32. Cumulative sum of snowfall in millimeters for Mount Rainier National Park per year.

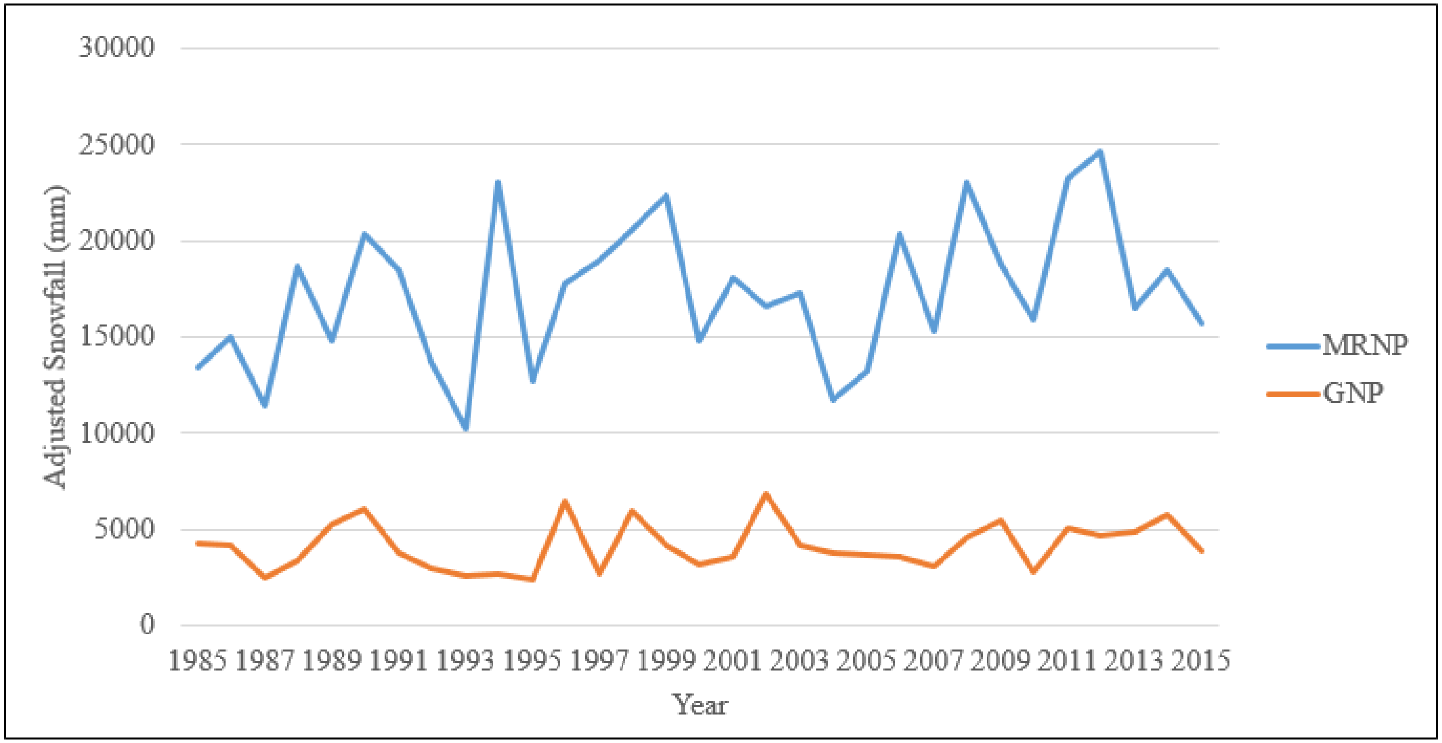

Figure 33. Comparison of snowfall totals between Glacier National Park and Mount Rainier National Park.

CONCLUSION

Glaciers in the Intermountain Region are undergoing ablation at a faster rate than glaciers in the Pacific Northwest partially because they have less snowfall and have higher positive degree day sums. This conclusion is based on the loss of a greater percentage of area in Glacier National Park, in addition to a larger loss of volume. However, not all of the ablation can be attributed to climatic factors. Outside the scope of this study, geologic factors distinguish the two regions as well. There are potentially different geothermal gradients between the two. Additionally, Mount Rainier has fumaroles, volcanic vents that release heated gases. Although there is some evidence of recent climate change between the regions that may be affecting glacial change, there are numerous other variables unaccounted for in this study that should be considered for attribution of glacial change including geology, seasonal weather variability, and localized anthropogenic activity.

Digital remote sensing and geographic information systems have select applications in glacier research. The amalgamation of the two are extremely useful when calculating glacier areas. This approach is however limited by the availability of cloud free satellite imagery. For example, the imagery useable for Glacier National Park was from mid-July in 1985 and from early October for 2000. This introduces seasonal variance between the two scenes. In mid-July, the glaciers would not have reached their yearly minimums yet, and by early October 2000, the first snowfall had already occurred. Therefore the same glacial conditions were not being compared. Further limitations occur with the presence of debris cover on the glaciers. The accuracy of the method depends on both the threshold value utilized when interpreting the NDSI and NDGI outputs as well as any human error induced from manually adjusting the vertices of the glacier boundaries to better match debris cover and glacier areas in shadow. However, five of the six years used in the project yielded accurate area results, and therefore if glacial area is the only parameter being evaluated, this method of quantifying spatial extent is effective.

Volume loss calculations however should not be performed based on digital remote sensing and GIS because of the limited historical data in existence. The quality of the historical topographic maps being used for the terrain of 1985 was poor, and the contour line intervals were 50 meters apart. The contour lines representing the terrain of 2015 were at 40 feet intervals, so they would allow for a more accurate representation of smaller differences in the terrain. Multiple errors were visibly detected within the older topographic maps when the contours were being traced; these errors included mislabeled lines and lines that disappeared completely. Ideally DEMs would have been used that had been based on radar technology, but they do not exist as historically as the project required.

In the future, researches may consider choosing a five year time span instead of a thirty year time frame and compiling multiple images from the ablation season for area calculations instead of relying on one image. This project was limited by being a desktop study, and would have benefitted to having a field component that allowed for ground truthing the glacier extents. Instead of using historical data, researchers could choose an individual glacier to study and build a weather station to monitor how a wider range of weather variables influence the glacier's ablation. It is a well-researched fact that some glaciers are melting, so another avenue for further research could be into ways to preserve and protect the glaciers.

LITERATURE CITED

Benn, D. and D. Evans. 2010. Glaciers and Glaciation. (2nd ed.) Routledge, New York, NY.

Bolch, T. 2013. Glacier Mapping and Monitoring. P. 1-9 in Proc. of. conf. on Advance Training Course in Land Remote Sensing. Harokopio University, Athens Greece. Available online at https://earth.esa.int/documents/10174/643007/D5P2b_TBolch__LTC2013.pdf; last accessed Jan. 09, 2020.

Bossler, J. 2010. Manual of Geospatial Science and Technology. (2nd ed.) Taylor and Francis, London.

Braithwaite R.J. and O.B. Olesen. 1989. Calculation of Glacier Ablation from Air Temperature, West Greenland. Glacier Fluctuations and Climatic Change. Glaciology and Quaternary Geology. 6: 219-233.

Campbell, J. and R. Wynne. 2011. Introduction to Remote Sensing. (5th ed.) The Guilford Press, New York, NY.

Crippen, R.E. 1988. The Dangers of Underestimating the Importance of Data Adjustments in Band Ratioing. International Journal of Remote Sensing. 9(4): 767–776.

Davies, B. 2017. Mapping the World's Glaciers. Available online at http://www.antarcticglaciers.org/glaciers-and-climate/glacier-recession/mapping-worlds-glaciers/; last accessed Jan. 10, 2019.

Fagre, D.B., L. McKeon, K. Dick, and A. Fountain. 2017. Glacier Margin Time Series (1966, 1998, 2005, 2015) of the Named Glaciers of Glacier National Park, MT, USA. Available online at https://www.sciencebase.gov/catalog/item/58af7022e4b01ccd54f9f542?community=Northern+Rocky+Mountain+Science+Center; last accessed Jan. 09, 2020.

Farinotti, D., M. Huss, J. Furst, J. Landmann, H. Machguth, F. Maussion, and A. Pandit. 2019. A Consensus Estimate for the Ice Thickness Distribution of All Glaciers on Earth. Nature Geoscience. 12: 168-173.

GIS Geography. 2019. Landsat Program: Satellite Imagery Data and Bands. Available online at https://gisgeography.com/landsat-program-satellite-imagery-bands/; last accessed Jul. 11, 2019.

Haeberli, W. and M. Beniston. 1998. Climate Change and Its Impacts on Glaciers and Permafrost in the Alps. Ambio. 27: 258-265.

Hall, D. and J. Martinec. 1985. Remote Sensing of Ice and Snow. Chapman and Hall, London. 189.

Hall, M. and D. Fagre. 2003. Modeled Climate-Induced Glacier Change in Glacier National Park, 1850-2100. BioScience. 53(2): 131-140.

Harris, C. and J. Murton. 2005. Interactions between Glaciers and Permafrost: an Introduction. Cryospheric Systems: Glaciers and Permafrost. Geological Society, London.

Heiskanen, J. 2002. Assessment of Glacier Changes and Mass Balance Using Landsat Satellite Data in Svartisen, Northern Norway. M.Sc. thesis, Department of Geography, University of Turku, Finland. In Finnish, English abstract, 148.

Hendriks, J. and P. Pellikka. 2007. Semiautomatic Glacier Delineation from Landsat Imagery over Hintereisferner Glacier in the Austrian Alps. Zeitschrift für Gletscherkunde und Glazialgeologie. 41: 55–75.

Kaser, G. 2001. Glacier-climate Interaction at Low Latitudes. Journal of Glaciology. 47: 195–204.

Key, C., D. Fagre, and R. Menicke. 2002. Glacier Retreat in Glacier National Park, Montana. P. J365–J376 in Satellite Image Atlas of Glaciers of the World, Williams, R. Jr, Ferrigno, J. (Eds.). US Government Printing Office, Washington (DC).US Geological Survey Professional Paper 1386J.

Kienholz, C., S. Herreid, J. L. Rich, A.A. Arendt, R. Hock, and E. Burgess. 2015. Derivation and Analysis of a Complete Modern-date Glacier Inventory for Alaska and Northwest Canada. Glaciology. 61(227): 403– 420.

Knap, W.H. 1997. Satellite Derived and Ground-based Measurements of the Surface Albedo of Glaciers. Ph.D. dissertation, University of Utrecht, The Netherlands, 175.

Kuhn, M. 2010. The Formation and Dynamics of Glaciers. Remote Sensing of Glaciers: Techniques for Topographic, Spatial and Thematic Mapping of Glaciers. CRC Press, London. 21-39.

Marston, R. A., L. O. Pochop, G. L. Kerr, and M. L. Varuska. 1989.Recent Trends in Glaciers and Glacier Runoff. Headwaters Hydrologic. Wind River Range, Wyoming. 159–169.

Martin S. 1974. Correlation Bilans de Masse Annuels—Facteurs Météorologiques dans les Grandes Rousses.Zeitschrift für Gletscherkunde. Glazialgeologie. 10: 89–100.

Mihalcea, C., B. Brock, G. Diolaiuti, C. D'Agata, M. Citterio, M. Kirkbride, M. Cutler, and C. Smiraglia. 2008. Using ASTER Satellite and Ground-based Surface Temperature Measurements to Derive Supraglacial Debris Cover and Thickness Patterns on Miage Glacier (Mont Blanc Massif, Italy). Cold Regions Science and Technology. 52(3): 341–354.

National Oceanic and Atmosphere Administration (NOAA). 2020. Global Historical Climate Network. Available online at https://www.ncdc.noaa.gov/cdo-web/datasets; last accessed Mar. 13, 2020.

National Park Service (NPS). 2009. Monitoring Glacial Features and Process. Available online at https://www.nps.gov/articles/glacier-monitoring-techniques.htm; last accessed Jan. 12, 2019.

National Park Service (NPS). 2017. Change in Glacial Extent at Mount Rainer National Park from 1896 to 2015. Available online at https://irma.nps.gov/DataStore/DownloadFile/580543; last accessed Jul. 3, 2019.

National Park Service (NPS). 2019. National Parks. Available online at http://catalog.data.gov/dataset/national-parks; last accessed Sep. 15, 2019.

National Snow and Ice Data Center (NSIDC). 2019). How Are Glaciers Formed?. Available online at https://nsidc.org/cryosphere/glaciers/questions/formed.html; last accessed May 18, 2019.

Nylen, T. 2004. Spatial and Temporal Variations of Glaciers (1913-1994) on Mt. Rainier and the Relation with Climate. M. Sc. Thesis, Portland State University.

Parcak, S. 2009. Satellite Remote Sensing for Archeology. Routledge, New York, NY.

Paterson, W. 1994. The Physics of Glaciers. (3rd ed). Butterworth-Heinemann, Oxford. 480.

Paul, F. and Hendriks. 2010. Optical Remote Sensing of Glacier Extent. Remote Sensing of Glaciers: Techniques for Topographic, Spatial and Thematic Mapping of Glaciers. CRC Press, London.

Paul, F., C. Huggel, A. Kääb, and T. Kellenberger. 2003. Comparison of TM-derived Glacier Areas with Higher Resolution Data Sets. In Proc. of the EARSeL Workshop on Remote Sensing of Land Ice and Snow, Berne, Switzerland, March 11–13, 2002. EARSeL eProceedings. 2: 15–21.

Paul, F., H. Machguth, and A. Kääb. 2005. On the Impact of Glacier Albedo under Conditions of Extreme Glacier Melt: the Summer of 2003 in the Alps. In Proc. of the EARSeL Workshop on Remote Sensing of Land Ice and Snow, Berne, Switzerland, February 21-23, 2005. EARSeL eProceedings. 4(2), 139–149.

Pellikka, P. and W. G. Rees. 2010. Glacier Parameters Monitored using Remote Sensing. Remote Sensing of Glaciers: Techniques for Topographic, Spatial and Thematic Mapping of Glaciers. CRC Press, London. 41-66.

Posamentier H. W. 1977. A New Climatic Model for Glacier Behavior of the Austrian Alps. Journal of Glaciology. 18: 57–65.

Racoviteanu, A., M. Williams, and G. Barry. 2008. Optical Remote Sensing of Glacier Characteristics: A Review with Focus on the Himalaya. Sensors. 8: 3355-3383.

Rees, W. G. 2010. Principles of Remote Sensing. Remote Sensing of Glaciers: Techniques for Topographic, Spatial and Thematic Mapping of Glaciers. CRC Press, London.

Richards, J. 2013. Remote Sensing Digital Image Analysis: an Introduction. (5th ed.) Springer- Verlag, Berlin Heidelberg.

Riedel, J. and R. Burrows. 2005. Long Term Monitoring of Small Glaciers at North Cascades National Park: a Prototype Park for the North Coast and Cascades Network. North Cascades National Park, Washington, 39.

Stohlgren, T. 1997. Rocky Mountains. Available online at http://web.archive.org/web/20060927145110/http://biology.usgs.gov/s+t/SNT/noframe/wm146.htm; last accessed Jul. 2, 2019.

United States Fish and Wildlife Service (USFWS). 2011. Climate Change in the Pacific Region. Available online at https://www.fws.gov/pacific/Climatechange/changepnw.html; last accessed Aug. 14, 2019.

United States Geologic Survey (USGS). 2019a. What is a glacier?. Available online at https://www.usgs.gov/faqs/what-a-glacier?qt-news_science_products=0#qt-news_science_products; last accessed Jun. 13, 2019.

United States Geologic Survey (USGS). 2019b. Landsat Satellite Missions. Available online at https://www.usgs.gov/land-resources/nli/landsat/landsat-satellite-missions?qt-science_support_page_related_con=2#qt-science_support_page_related_con; last accessed Jun. 28, 2019.

United States Geologic Survey (USGS). 2019c. What are the Band Designations for the Landsat Satellites? Available online at https://www.usgs.gov/faqs/what-are-band-designations-landsat-satellites?qt-news_science_products=0#qt-news_science_products; last accessed Jun. 28, 2019.

United States Geologic Survey (USGS). 2019d. Retreat of Glaciers in Glacier National Park. Available online at https://www.usgs.gov/centers/norock/science/retreat-glaciers-glacier-national-park?qt-science_center_objects=0#qt-science_center_objects; last accessed Jul. 10, 2019.

United States Geologic Survey (USGS). 2019e. Earth Explorer. Available online at http://earthexplorer.usgs.gov; last accessed Sep. 15, 2019.

United States Geologic Survey (USGS). 2020a. The National Map. Available online at http://viewer.nationalmap.gov/basic; last accessed Mar. 10, 2020.

United States Geologic Survey (USGS). 2020b. TopoView. Available online at http://ngmdb.usgs.gov/topoview/viewer; last accessed Feb. 25, 2020.

Wastlhuber, R., R. Hock, C. Kienholz, and M. Braun. 2017. Glacier Changes in the Susitna Basin, Alaska, USA, (1951–2015) Using GIS and Remote Sensing Methods. Remote Sensing. 9(5): 478.

Waterman, J. 2019. Imagine Mount Rainier without its Icy Mantle. Available online at https://www.seattletimes.com/opinion/imagine-mount-rainier-with-a-lowercase-r-an-ode-to-our-disappearing-glaciers/; last accessed Mar. 10, 2020.

World Glacier Monitoring Service (WGMS). 2008. Global Glacier Changes: Facts and Figures. United Nations Environment Programme. Available online at https://wgms.ch/downloads/published/other_reports/wgms_2008_ggc.pdf; last accessed May 18, 2019.

VITA

Brianna Clark received her Associates Degree in General Studies in 2015 from San Jacinto Community College in Houston, TX. She graduated with her Bachelor of Arts in English with a minor in Environmental Science from Stephen F. Austin State University in 2017. Brianna spent a year in South Korea teaching English as a Second Language to secondary education students. In Fall 2018, she returned to the United States to pursue a Master of Science in Environmental Science with a minor in Spatial Science. She completed her master's from Stephen F. Austin in May 2020, and she plans to begin a Doctorate of Philosophy in Forestry starting Fall 2020.

Permanent Address: 2377 Indigo Harbour Ln.
League City, TX 77573

Style of Journal of Forestry

This thesis was typed by Brianna Clark.